Article
JOURNAL OF UNIVERSITY OF BABYLON
For Pure and Applied Sciences (JUBPAS)
Vol. 34 ; No.2 | 2026

A Trigonometric Function-Based Algorithm for CT-Scan Image Color Enhancement

Batool T. Altaee [1*], Kawther H. Al-khafaji [2]
[1]College of Education for Women, University of Kufa, batoolt.altaee@student.uokufa.edu.iq, Babylon, city center, Iraq.
[2]College of Education for Women, University of Kufa, Kutherh.kafajy@uokufa.edu.iq, Najaf, city center, Iraq.
***Corresponding author email:** batoolt.altaee@student.uokufa.edu.iq; mobile: 07818919069

خوارزمية تعتمد على الدوال المثلثية لتحسين ألوان صور الأشعة المقطعية

بتول ثابت كاظم [1*] كوثر حسن صاحب[2]

1 كلية التربية للبنات ، جامعة الكوفة ، batoolt.altaee@student.uokufa.edu.iq ، بابل، العراق
2 كلية التربية للبنات ، جامعة الكوفة ،Kutherh.kafajy@uokufa.edu.iq ، النجف، العراق

Accepted: 17/5/2026 **Published:** 30/6/2026

ABSTRACT

The rapid advancement of medical technologies has led to a substantial increase in the acquisition and storage of medical images, particularly through techniques such as computed tomography (CT). This growth highlights the need for effective image processing algorithms that can support physicians in diagnosing and evaluating medical conditions more efficiently. Among these approaches, medical image colorization has attracted growing interest in recent years. Unlike traditional grayscale images, synthesized color images can provide enhanced visual information about organs and tissues, thereby improving image interpretation. In this study, a novel mathematical approach is proposed to enhance the quality of CT scan images using trigonometric functions governed by three main parameters, using MATLAB software. The experimental results demonstrate that improving color contrast contributes to a more accurate distinction between different tissues and organs, offering clearer visual representation and supporting analytical as well as diagnostic processes. The evaluation by radiology experts indicated a significant improvement in the quality of the enhanced images, supporting the quantitative assessment results and confirming the effectiveness of the proposed method.

Keywords: CT-Scan**,** A Trigonometric Function, Image Enhancement, Color Image, MATLAB

ISSN: 2312-8135 | Print ISSN: 1992-0652
info@journalofbabylon.com | jub@itnet.uobabylon.edu.iq | www.journalofbabylon.com

ISSN: 2312-8135 | Print ISSN: 1992-0652

info@journalofbabylon.com | jub@itnet.uobabylon.edu.iq | www.journalofbabylon.com

1. INTRODUCTION

Medical imaging is vital for finding diseases and keeping track of how well treatments are working, but medical images aren't always clear. Medical photos can be fuzzy or weak for several reasons, including emergencies, loud environments, patient limits, lighting issues, and equipment constraints. This is because medical images are exceedingly complicated because they show many layers of the body at once. Image-enhancing techniques are extremely important when you can't take pictures again. These methods help doctors see better. Because of the limits of the equipment used to take these pictures, they often have bad contrast. This makes it much harder for a doctor to read the picture. [3] The main purpose of image enhancement is to change the image such that we can see and understand the visual information it contains more clearly. So, image enhancement is somewhat subjective because it depends a lot on what kind of information the viewer wants to get from the image. [4] Image enhancement is the process of making an image look better by changing the brightness, contrast, and quality of the picture. The literature has suggested several traditional ways to improve the visual representation of medical pictures by boosting the contrast and picture quality and reducing noise. [5] The best approach to improve an image is to change its color. Medical imaging is particularly important for finding problems with the interior organs [6]. Most of the medical photographs we obtain are either black and white or grayscale. We can see millions of hues, but only a few shades of gray. So, we need to color them so that we can see the pictures clearly. Adding colors to pictures makes them easier to grasp. For example, in medical photographs, you can see even small bones and tissues clearly. We need to color the medical pictures, then. [7] Color can be a very crucial clue for finding shapes and items. The radiologist can better understand the images when their detecting capacity is up, which helps them recognize objects and provide more accurate diagnoses. An observer can only see about 140 levels of gray, but a well-colored image can let a user see 250 to 1000 levels, which means that the image's features can be detected 2 to 7 times more easily. Colorizing medical photos can be utilized for many different diagnostic applications, making it a useful tool for visualizing data. [8]

Although previous studies have relied on trigonometric functions with fixed, defined coefficients, this study presents a systematic analysis of the effect of changing the three coefficients (F, P, N) individually and collectively. This approach allows for a deeper understanding of the behavior of the functions and their impact on image enhancement properties, in terms of intensity and contrast distribution, which has not been addressed in detail in previous studies.

2. MEDICAL IMAGES

Involves imaging of different sections of the body, like bones, organs, and tissues, that are then used for medical research and therapy of patients. Medical imaging employs essential physical phenomena, ranging from acoustic wave transmission to X-ray propagation, to assess patient health characteristics. In the past, medical imaging just showed how structures looked. Now, they can also look at complex biological processes in the body, such as mutation, metabolism, blood flow, chemical interactions, and more. Medical imaging not only aids in disease diagnosis but also enhances the study of human anatomy and the evaluation of drug chemical reactions. [9] The most popular kinds are:

ISSN: 2312-8135 | Print ISSN: 1992-0652
info@journalofbabylon.com | jub@itnet.uobabylon.edu.iq | www.journalofbabylon.com

2.1 Computed Tomography Images (CT)

It is a way to take pictures of the body that employs X-rays and complex computer algorithms to make detailed cross-sectional pictures. [10] The CT image is made by moving the X-ray tube around the body such that x-rays pass through it at different locations. At least one direct-identifier cluster faces the X-beam source to collect information about the transmission projection. A computer puts together all the many pieces of information it gets this way to make a tomographic image of the patient. [11] Computed tomography (CT) uses high-energy X-rays, which might give some people a lot of radiation. CT imaging is great for seeing bone structures and finding traumatic injuries since it has excellent spatial resolution and can be done quickly. This makes it very useful in emergencies. But its utility is limited by exposure to ionizing radiation, which can be dangerous, especially for people who are already sick. [13]

3. HISTORY AND FUTURE OF IMAGE ENHANCEMENT

The evolution of digital image processing is closely related to the advancement of digital computing technology. Digital images need a lot of storage and processing power; therefore, progress in digital image processing has depended on the growth of digital computers and technologies that support them, such as data storage, display, and transport. In the early 1960s, the first computers that could do useful image processing tasks came out. In 1964, the Jet Propulsion Laboratory started working on ways to use computers to improve photographs from space probes. This was when a computer was used to fix different types of image distortion that were common in the onboard television camera by processing pictures of the moon sent by Ranger 7. Digital image processing techniques started being applied in astronomy, medical imaging, and distant Earth resources observations in the late 1960s and early 1970s, along with space applications. The development of computerized axial tomography (CAT), or computerized tomography (CT) for short, in the early 1970s is one of the most important developments in the use of image processing for medical diagnosis. [14] Recently, computer vision and artificial intelligence technologies have gotten better, and machine learning, especially deep learning models, has become the main way to analyze medical images. Deep learning has not only produced impressive outcomes in image classification, segmentation, and lesion identification but has also accelerated the advancement of computer-aided diagnostic (CAD) systems. [15]

4. IMAGE QUALITY METRICS

Image Quality Metrics (IQMs) play a crucial role in the development and evaluation of image processing algorithms, as they provide a quantitative means to assess the performance of processed images [16]. A variety of image quality assessment measures are commonly employed due to their simplicity in computation, clear physical interpretation, and ease of integration within mathematical optimization frameworks. [17] Many of these techniques are widely used and will be explained as follows.

4.1 Peak Signal to Noise Ratio

For the measurement of reconstruction quality, PSNR is one of the most extensively used metric parameters. It describes the ratio of the maximum possible power of a signal to the power of corrupting noise and is normally represented in decibel scale. PSNR values typically range between (20 – 50) db. Higher values indicate greater similarity between the processed and original image and a lower level of distortion, while lower values indicate greater differences and loss of quality. PSNR can be expressed as follows:[18]

ISSN: 2312-8135 | Print ISSN: 1992-0652 | www.journalofbabylon.com | jub@itnet.uobabylon.edu.iq | info@journalofbabylon.com

$$\text{PSNR (dB)}=10 \times \log_{10} \frac{(2n-1)^2}{\text{MSE}} \quad \ldots. (1)$$

4.2 Edge Strength Similarity Image Metric (ESSIM)

It is an objective measure of edge similarity between the original and processed images. ESSIM measures the structural similarity between the original and processed image. produces values in the range [0, 1], where values closer to 1 indicate a higher similarity in edge structure between the original and processed images, while values closer to 0 indicate significant structural distortion. It is calculated according to the equation:[19]

$$ESSIM(f,g) = \frac{1}{N}\sum_{i=1}^{N} \frac{2E(f,i)E(g,i)+C}{(E(f,i))^2+(E(g,i))^2+C} \quad \ldots. (2)$$

4.3 Entropy

It is a statistical measure of randomness that can be used to characterize the texture of the input image. High entropy values in the processed image compared to the original indicate increased detail or randomness, while low values indicate loss of some detail or simplification of the image content. The information entropy is an evaluation of the uncertainty degree in the system, which can be expressed mathematically by the equation**:** [20]

$$\text{Entropy(IE)} = \sum_{x=0}^{255} \left[P(x) \times \log_2 \left(\frac{1}{P(x)} \right) \right] \quad \ldots. (3)$$

5. MATHEMATICAL ANALYSIS

In a color model, a new pixel has three RGB channels, each with a value that is between 0 and 1. Three different functions change these channels to get the final color of the image based on the type of transformation. In this kind of image enhancement, we represent the right part ($2\pi f\ I_Z\ (x, y)$) for all of the triple equations, which are parts of the main equation (1), in terms of trigonometric functions (sine, cosine, tangent). A wide variety of practical enhanced image results can be obtained. The general formulas for the experimental coloring equations are:

$$I_E(x,y) = \begin{bmatrix} |2\pi\mathcal{F}I_z(x,y))| \\ |2\pi\mathcal{F}I_z(x,y)+NP)| \\ |2\pi\mathcal{F}I_z(x,y)+P)| \end{bmatrix} \quad \ldots (4)$$

Where, $I_E(x,y)$: The output colouring image.

$I_z(x,y)$: The initial processed image.

F:The frequency coefficient.

P: the phase coefficient.

N:The Optional empirical coefficient.

ISSN: 2312-8135 | Print ISSN: 1992-0652 | www.journalofbabylon.com | jub@itnet.uobabylon.edu.iq | info@journalofbabylon.com

6. IMAGE ACQUISITION

The medical image utilized in this study paper is a computed tomography (CT) scan depicting a cross-section of the upper abdomen, measuring 540 x 539. We used a Windows 10 laptop with MATLAB 2023 to accomplish all of the digital simulations and data analysis.

7. STEPS OF THE PROPOSED COLORING ALGORITHM

Step 1: Loading image: A sample medical image, such as a CT scan image, is selected and loaded using the uigetfile function during this stage.
Step 2: Intensity adjustment of images: Contrast and lighting within the image are enhanced to show tissues and medical details more clearly using the (imadjust) function.
Step 3: Convert the resulting image to a double-precision image
Step 4. Initial Enhancing: This stage is used to remove noise and refine important edges and details before applying mathematical equations.
Step 5. Choosing a mathematical function: Choosing the appropriate mathematical equation to convert a grayscale image to a color image and improve color distribution (sine, cosine, tangent)
Step 6. Input three parameters**:** Control parameters that affect the distribution of colors and the shape of the resulting image (F, P, N) are entered**.**
Step 7. Expression of the original image in terms of the parameters: The original image is combined with the coefficients within the mathematical equation to form the final mathematical model.
Step 8. Bind a variable parameter experimentally to the image: Experiment with different values for the parameters in order to achieve the best color gradient and visual improvement for the medical image.
Step 9. Apply experimental equation with the parameter: Mathematical equations are implemented to generate the three-color channels (RGB) of a color image.
Step 10. Coloring medical images: RGB color channels are combined, and the resulting color image is displayed to improve the visibility of medical details.

Figure 1. illustrates the flow chart of the basic algorithm stages:

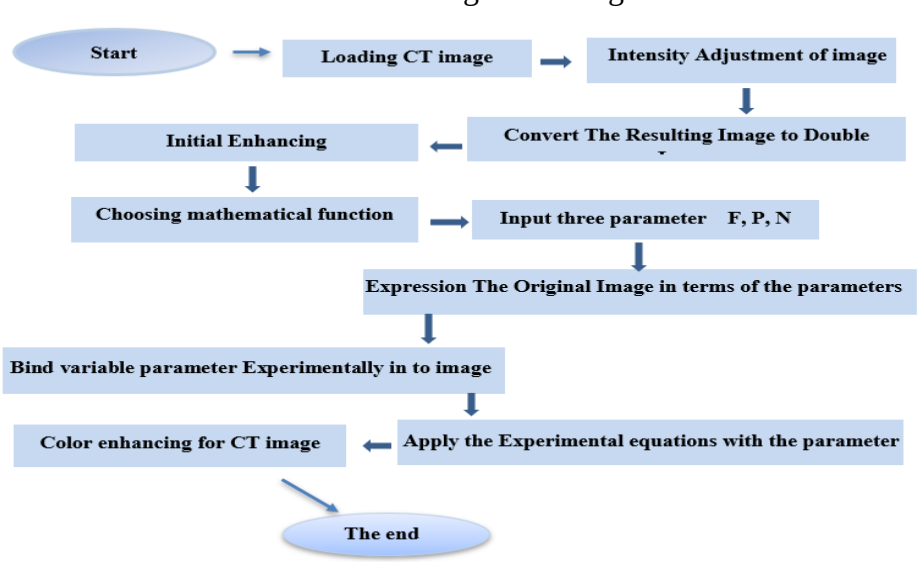

Fig.1 Flowchart of propose algorithm

ISSN: 2312-8135 | Print ISSN: 1992-0652
info@journalofbabylon.com | jub@itnet.uobabylon.edu.iq | www.journalofbabylon.com

8. EXPERIMENTAL RESULTS OF MEDICAL IMAGES

A mathematical algorithm based on an empirical equation using trigonometric functions (sine, cosine, tangent) based on Fourier transforms on three main coefficient frequencies (F), phase (P), and the optional empirical coefficient (N) was applied to a computerized tomography (CT) image. The experimental study revealed that any change in the values of these parameters produced different results each time they were modified. The results of these functions can be shown as follows:

1. Results of coloring CT-scan images for the sin function

1.1. The parameters (N) and (P) were constant at 0.2 and 0.5, respectively, the value of the coefficient F was varied within the range of (0.2–0.8)

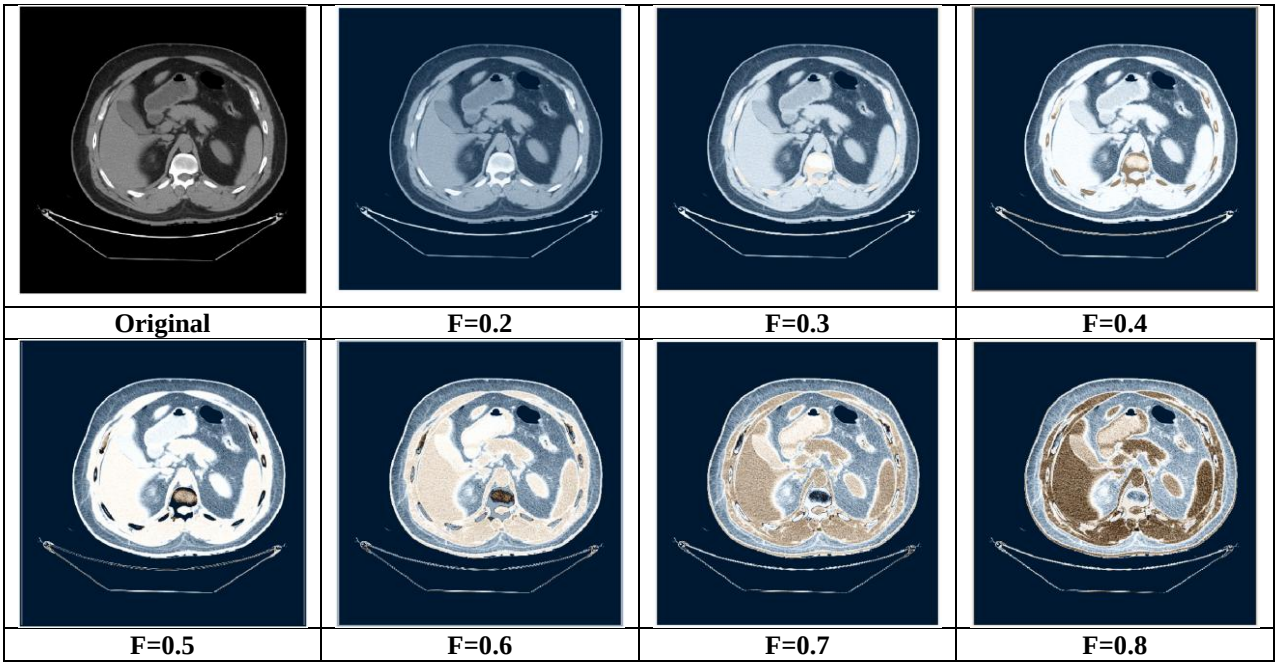

Fig.2 The color output CT-Scan images with different F values

1.2. The parameters (F) and (P) were constant at 0.9 and 0.2, respectively, the value of the coefficient N was varied within the range of (0.1–0.9)

ISSN: 2312-8135 | Print ISSN: 1992-0652
info@journalofbabylon.com | jub@itnet.uobabylon.edu.iq | www.journalofbabylon.com

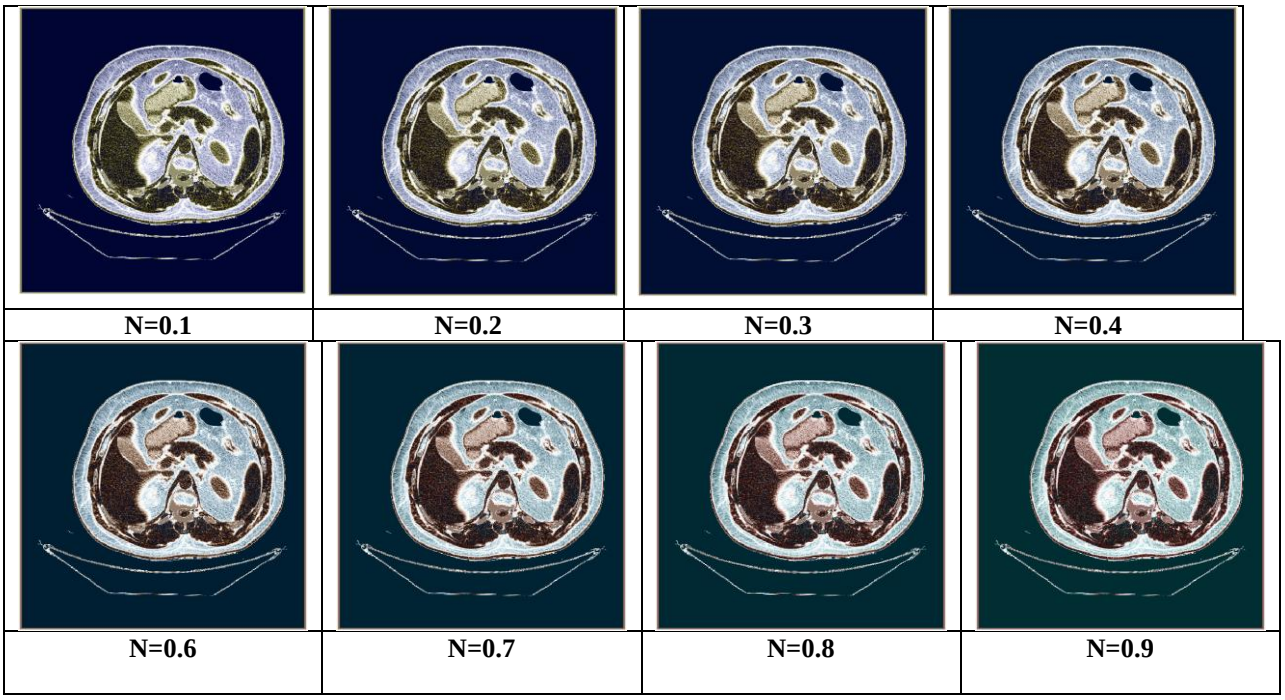

Fig.3 The color output CT-Scan images with different N values

1.3. The value of the coefficient (P) was varied within the range of (0.3–1), while coefficients F and N were kept constant at 0.9 and 0.5, respectively.

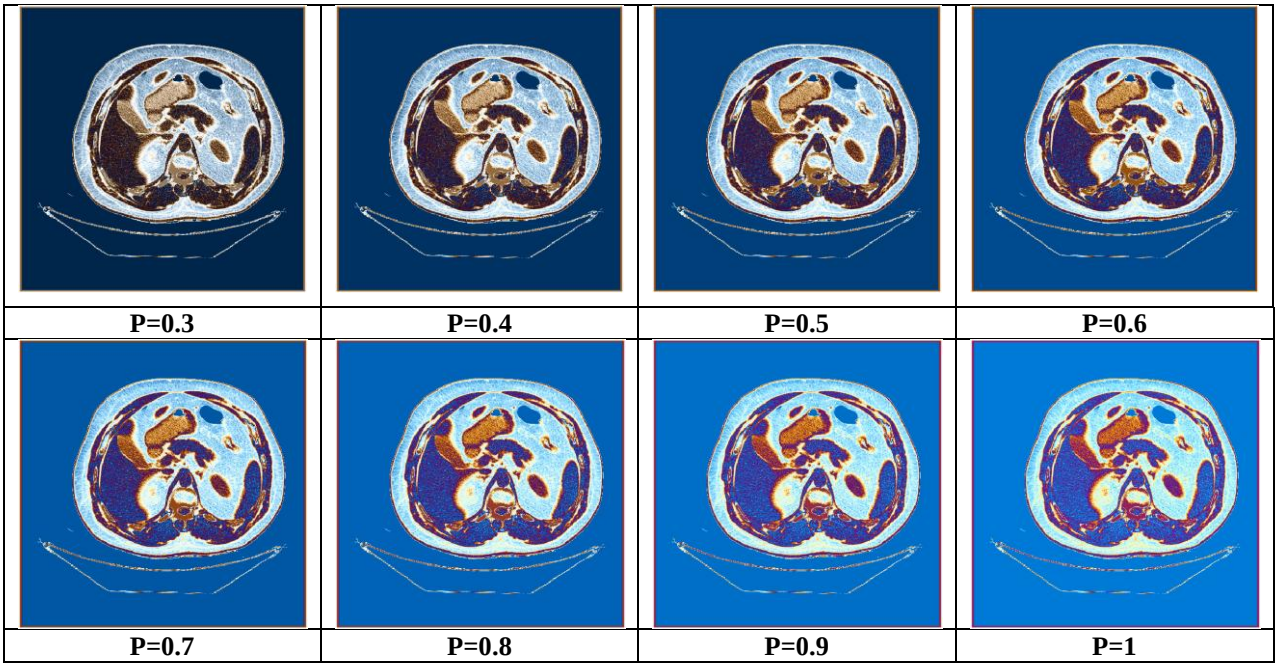

Fig.4 The color output CT-Scan images with different P values

1.4. The coefficients (F) and (N) were varied simultaneously within the ranges of (0.3–1) and (0.1–0.9), respectively, while coefficient (N) was kept constant at (0.5).

ISSN: 2312-8135 | Print ISSN: 1992-0652
info@journalofbabylon.com | jub@itnet.uobabylon.edu.iq | www.journalofbabylon.com

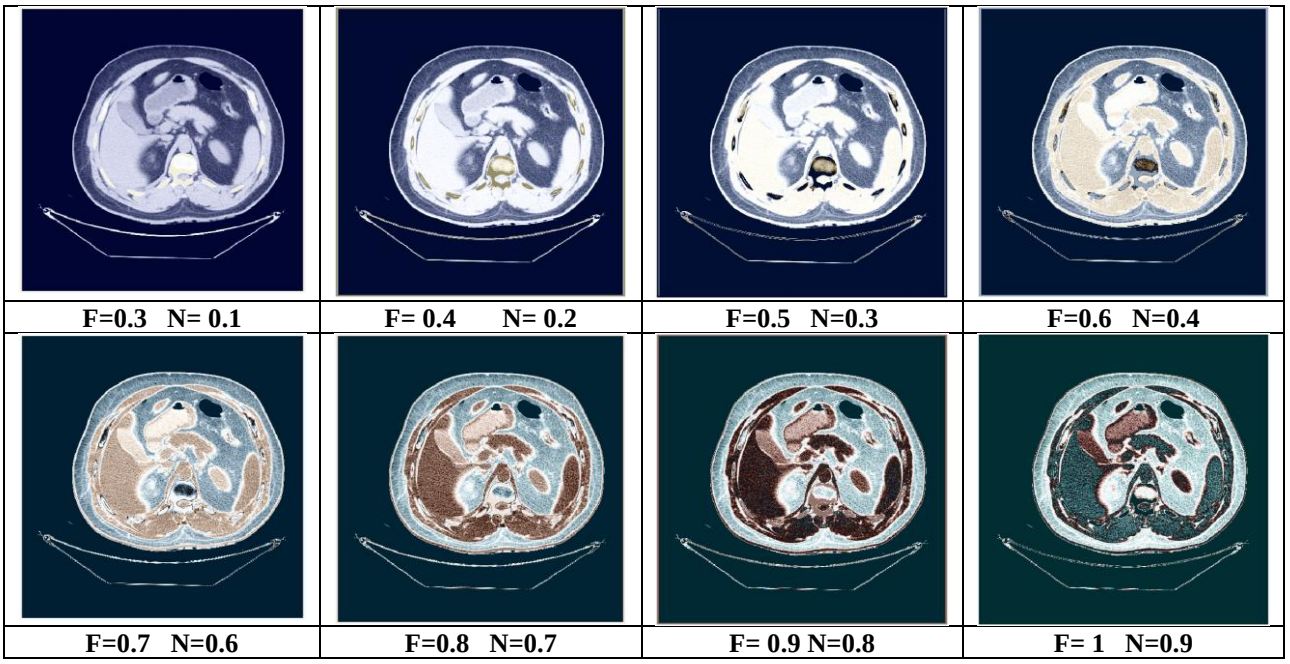

Fig.5 The color output CT-Scan images with different F and N values

1.5. When the values of coefficients F and P were adjusted across the ranges (1–2.4) and (0.4 – 1.8), respectively, while the value of coefficient (N) remained unchanged at 0.5.

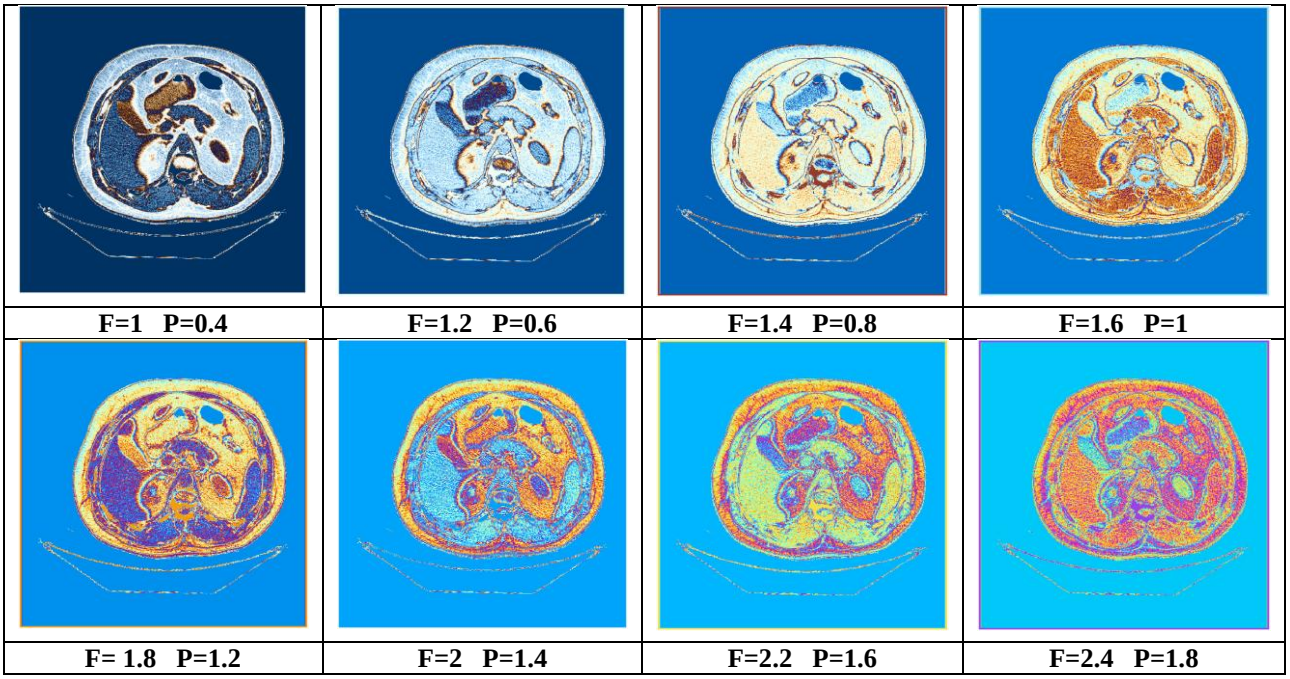

Fig.6 The color output CT-Scan images with different F and P values

1.6. Changing the values of both coefficients (N) and (P) to take a different set of values, and at the same time leaving the coefficient value (F) without changing, where it takes the value (0.9).

ISSN: 2312-8135 | Print ISSN: 1992-0652
info@journalofbabylon.com | jub@itnet.uobabylon.edu.iq | www.journalofbabylon.com

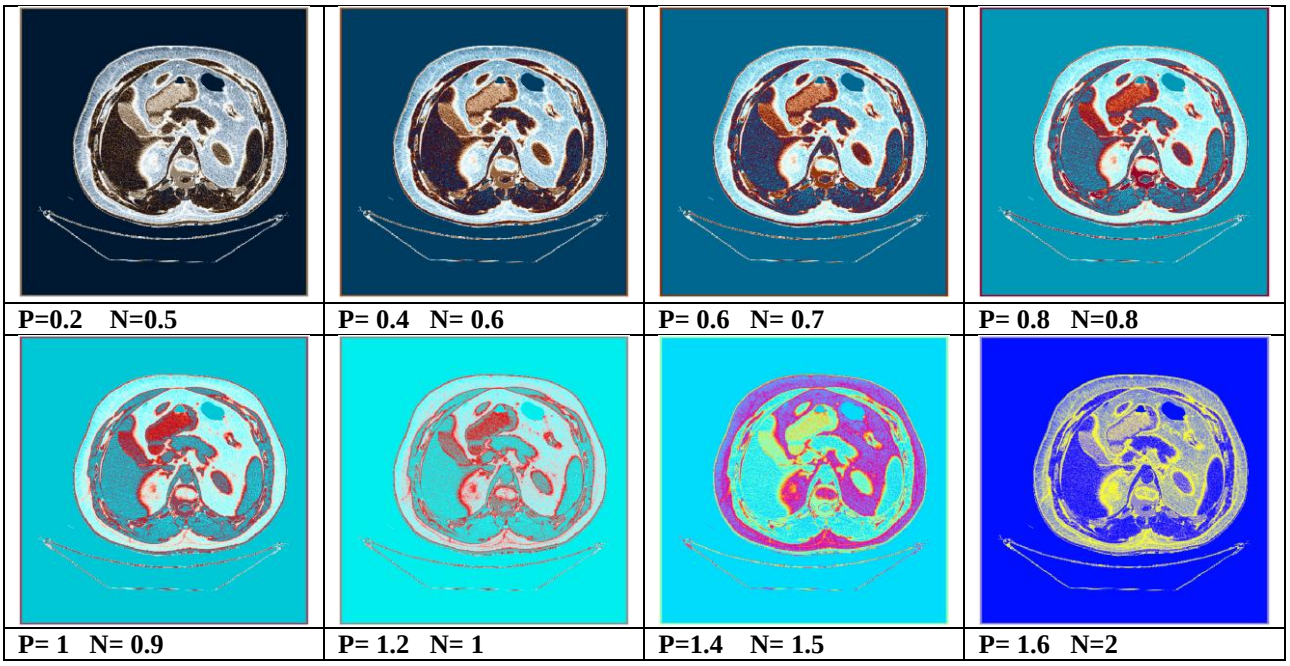

Fig.7 The color output CT-Scan images with different P and N values

1.7. When the three coefficients (F, P, N) are altered concurrently.

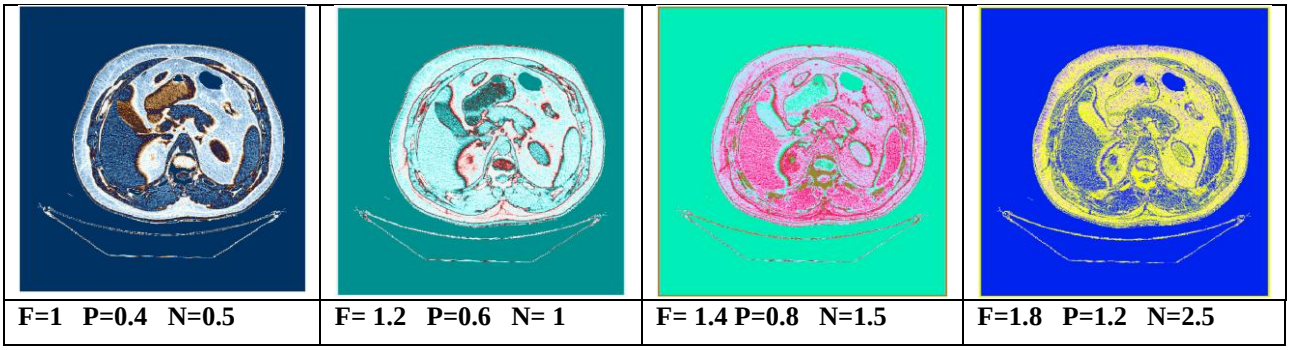

Fig.8 The color output CT-Scan images with different F, P, N values

Table (1) Quality Metrics for CT-Scan when the change coefficient F

IMQ	F=0.2	F=0.3	F=0.4	F=0.5	F=0.6	F=0.7	F=0.8
PSNR	13.57234	11.26990	9.553805	8.711385	9.323957	9.592001	9.316837
ESSIM	0.989923	0.989936	0.989820	0.989646	0.989850	0.989961	0.990002
E_O	3.846326	3.846326	3.846326	3.846326	3.846326	3.846326	3.846326
E_E	3.779950	3.705690	3.411867	3.359153	3.682435	3.479990	3.565891

Table (2) Quality Metrics for CT-Scan when the change coefficient N

IMQ	N=0.1	N=0.2	N=0.3	N=0.4	N=0.6	N=0.7	N=0.8	N=0.9
PSNR	8.48830	8.48830	8.48830	8.48830	8.48830	8.48830	8.48830	8.48830
ESSIM	0.98984	0.98984	0.98984	0.98984	0.98984	0.98984	0.98984	0.98984
E_O	3.84633	3.84633	3.84633	3.84633	3.84633	3.84633	3.84633	3.84633
E_E	3.74331	3.74331	3.74331	3.74331	3.74331	3.74331	3.74331	3.74331

ISSN: 2312-8135 | Print ISSN: 1992-0652
info@journalofbabylon.com | jub@itnet.uobabylon.edu.iq | www.journalofbabylon.com

Table (3) Quality Metrics for CT-Scan when the change coefficient P

IMQ	P=0.3	P=0.4	P=0.5	P=0.6	P=0.7	P=0.8	P=0.9	P=1
PSNR	7.43865	6.45079	5.54275	4.710114	4.08118	3.53315	3.05131	2.64133
ESSIM	0.98973	0.98978	0.98982	0.98986	0.98987	0.98988	0.98989	0.98989
E_O	3.84633	3.84633	3.84633	3.84633	3.84633	3.84633	3.84633	3.84633
E_E	3.73570	3.69004	3.66231	3.65466	3.60967	3.57644	3.56534	3.58748

Table (4) Quality Metrics for CT-Scan when changing the coefficient F, N

IMQ	F=0.3 N= 0.1	F= 0.4 N= 0.2	F=0.5 N=0.3	F=0.6 N=0.4	F=0.7 N=0.6	F=0.8 N=0.7	F= 0.9 N=0.8	F= 1 N=0.9
PSNR	11.2699	9.55381	8.71138	9.32396	9.592001	9.31684	8.48830	8.29849
ESSIM	0.98994	0.98982	0.98965	0.98985	0.98996	0.99000	0.98984	0.98968
E_O	3.84633	3.84633	3.84633	3.84633	3.84633	3.84633	3.84633	3.84633
E_E	3.70569	3.41187	3.35915	3.68244	3.47999	3.56589	3.74331	3.56502

Table (5) Quality Metrics for CT-Scan when change coefficient F, P

IMQ	F=1 P=0.4	F=1.2 P=0.6	F=1.4 P=0.8	F=1.6 P=1	F=1.8 P=1.2	F=2 P=1.4	F=2.2 P=1.6	F=2.4 P=1.8
PSNR	6.71037	4.94156	3.59165	2.99072	2.27325	2.03552	1.80763	2.04362
ESSIM	0.98962	0.98979	0.98982	0.98978	0.98999	0.98973	0.98999	0.98983
E_O	3.84633	3.84633	3.84633	3.84633	3.84633	3.84633	3.84633	3.84633
E_E	3.43079	3.34720	3.44658	3.59516	3.73551	3.48863	3.51433	3.69123

Table (6) Quality Metrics for CT-Scan when change coefficient N, P

IMQ	P=0.2 N=0.5	P=0.4 N=0.6	P= 0.6 N=0.7	P=0.8 N=0.8	P=1 N=0.9	P=1.2 N=1	P=1.4 N=1.5	P= 1.6 N=2
PSNR	8.48830	6.45079	4.71011	3.53315	2.64133	2.04882	1.76101	1.73514
ESSIM	0.98984	0.98978	0.98986	0.98988	0.98989	0.98990	0.98989	0.98987
E_O	3.84633	3.84633	3.84633	3.84633	3.84633	3.84633	3.84633	3.84633
E_E	3.74331	3.69004	3.65466	3.57644	3.58748	3.60839	3.51708	3.36569

Table (7) Quality Metrics for CT-Scan when change coefficient F, P, N

IQM	F=1 P=0.4 N=0.5	F=1.2 P=0.6 N= 1	F=1.4 P=0.8 N=1.5	F=1.8 P=1.2 N=2.5
PSNR	6.710373	4.941555	3.591653	2.273255
ESSIM	0.989623	0.989799	0.989817	0.989987
E_O	3.846326	3.846326	3.846326	3.846326
E_E	3.430792	3.347200	3.446576	3.735511

ISSN: 2312-8135 | Print ISSN: 1992-0652
info@journalofbabylon.com | jub@itnet.uobabylon.edu.iq | www.journalofbabylon.com

2. RESULTS OF COLORING CT-SCAN IMAGES FOR THE COSINE FUNCTION

2.1. The parameters (N) and (P) were constant at 0.2 and 0.5, respectively, the value of the coefficient F was varied within the range of (0.2–0.8)

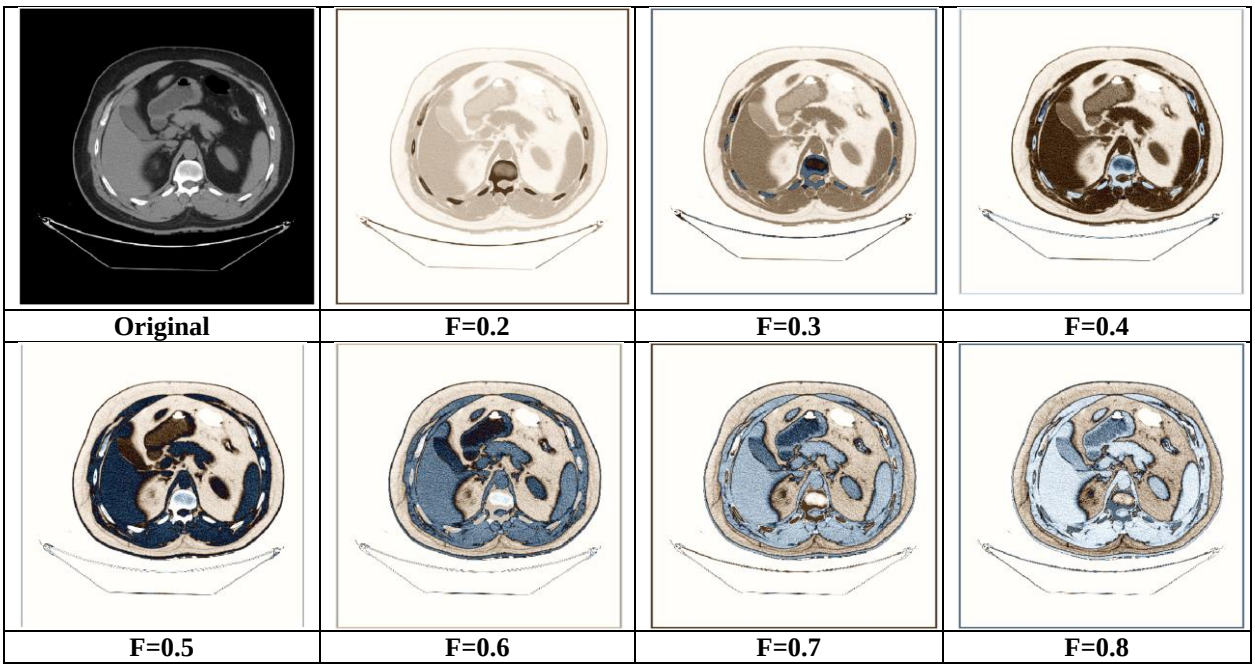

Fig.9 The color output CT-Scan images with different F values

2.2. The parameters (F) and (P) were constant at 0.9 and 0.2, respectively, the value of the coefficient N was varied within the range of (0.1–0.9)

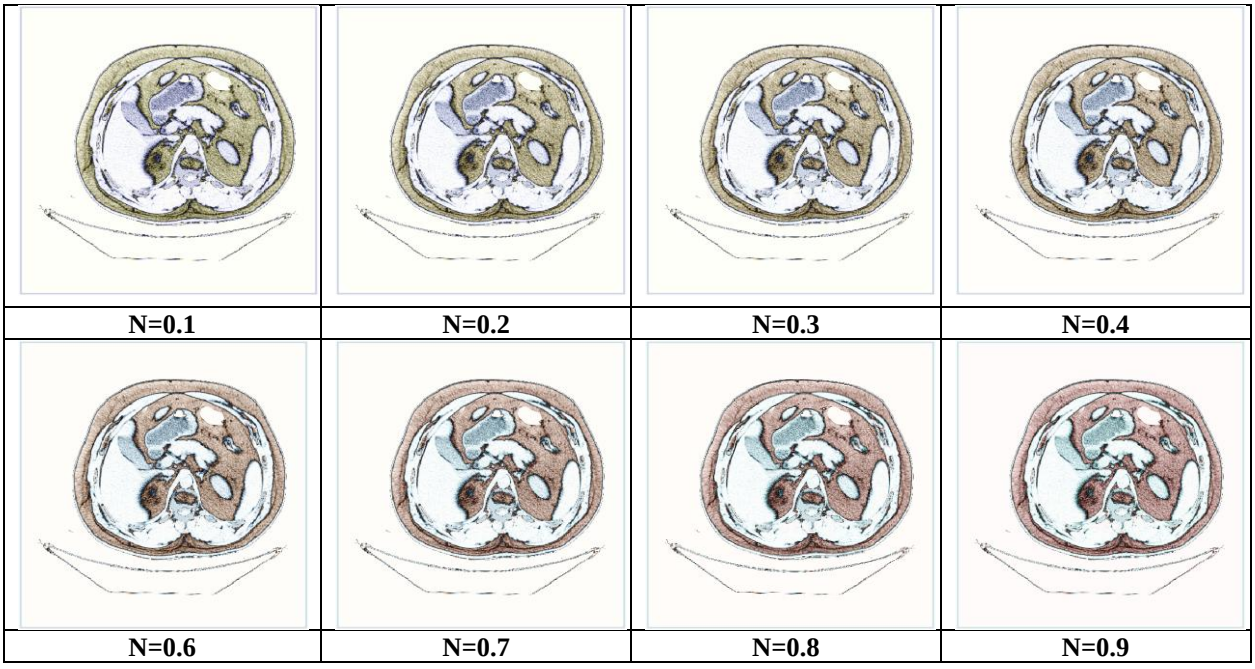

Fig.10 The color output CT-Scan images with different N values

ISSN: 2312-8135 | Print ISSN: 1992-0652
info@journalofbabylon.com | jub@itnet.uobabylon.edu.iq | www.journalofbabylon.com

2.3. The value of the coefficient (P) was varied within the range of (0.3–1), while coefficients F and N were kept constant at 0.9 and 0.5, respectively.

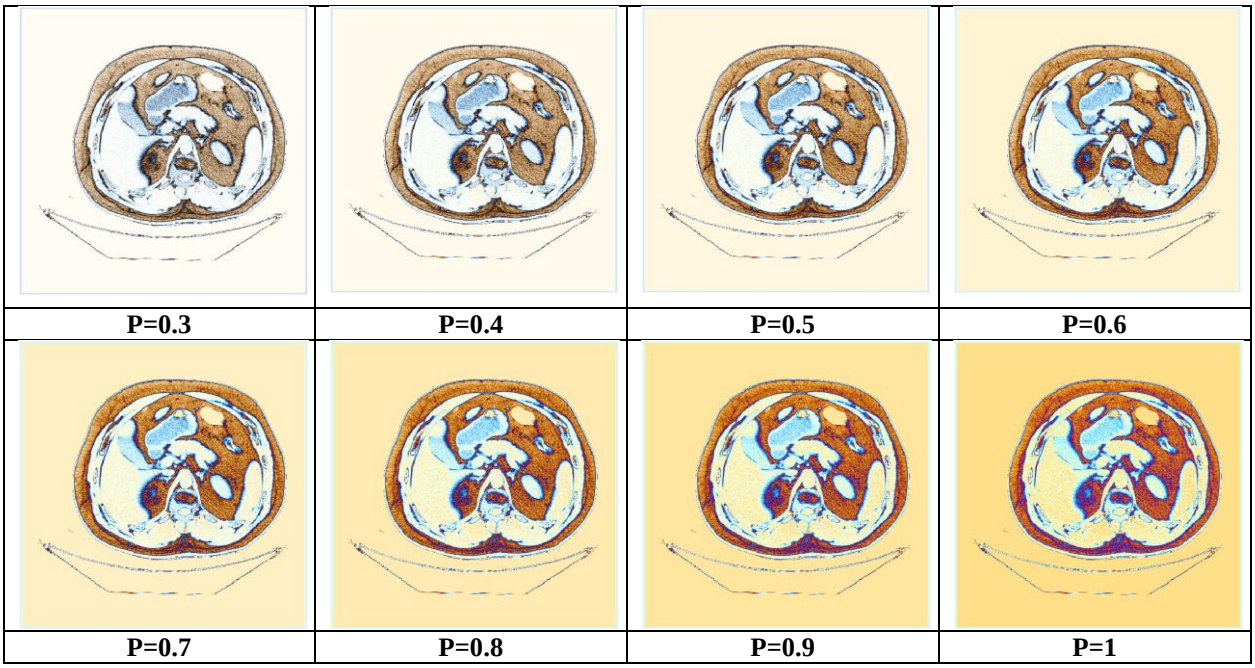

Fig.11 The color output CT-Scan images with different P values

2.4. The coefficients (F) and (N) were varied simultaneously within the ranges of (0.3–1) and (0.1–0.9), respectively, while coefficient (N) was kept constant at (0.5).

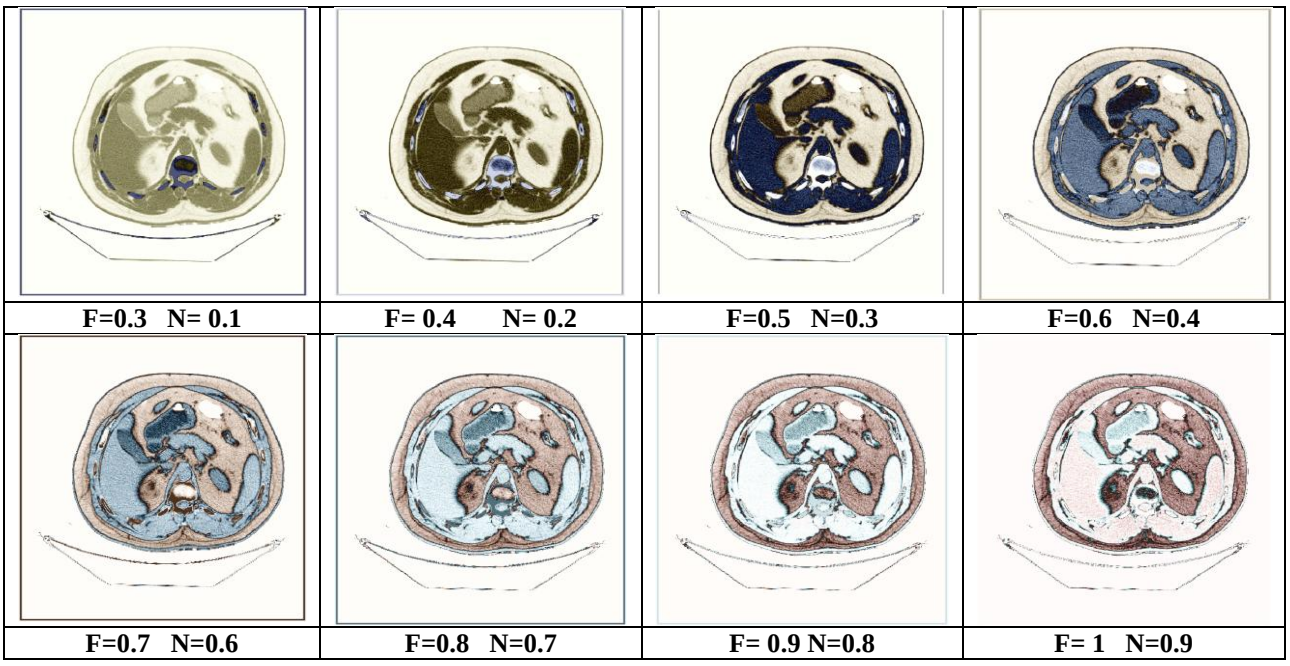

Fig 12 The color output CT-Scan images with different F and N values

مجلة جامعة بابل للعلوم الصرفة والتطبيقية مجلة جامعة بابل للعلوم الصرفة والتطبيقية

2.5. When the values of coefficients F and P were adjusted across the ranges (1–2.4) and (0.4 – 1.8), while the value of coefficient (N) remained unchanged at 0.5.

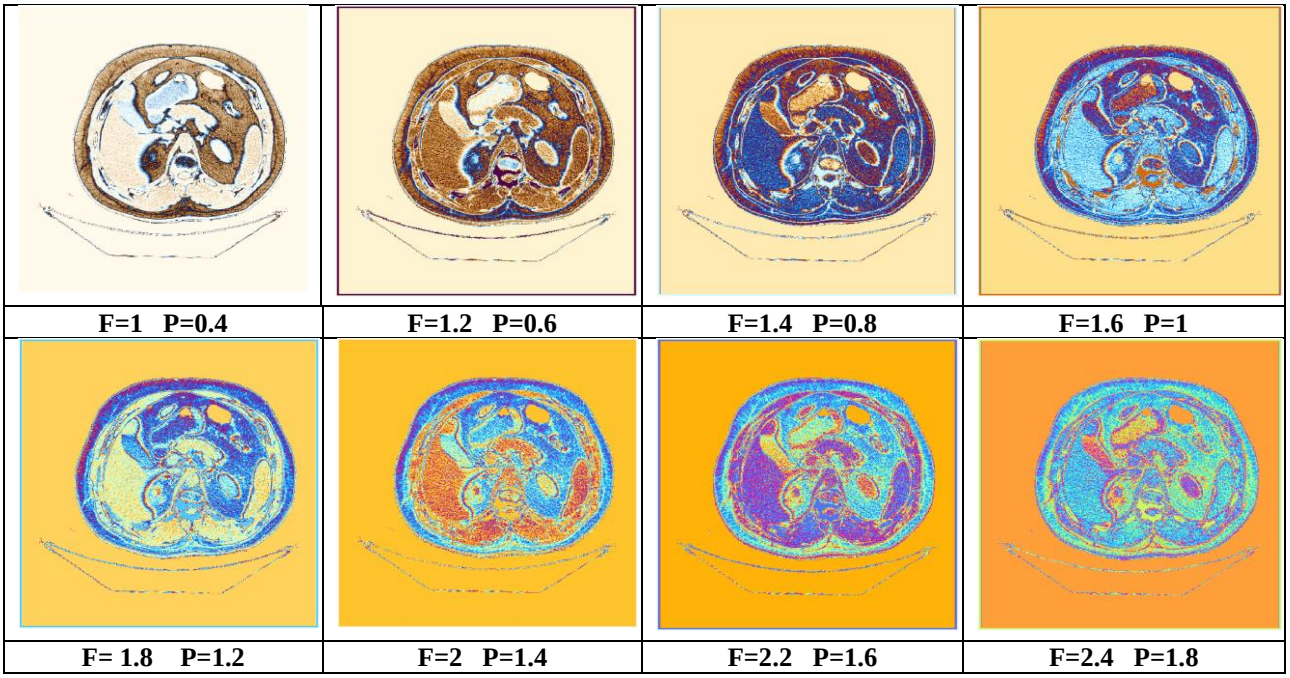

Fig 13 The color output CT-Scan images with different F and P values

2.6. Changing the values of both coefficients (N) and (P) to take a different set of values and at the same time leaving the coefficient value (F) without changing, where takes the value (0.9).

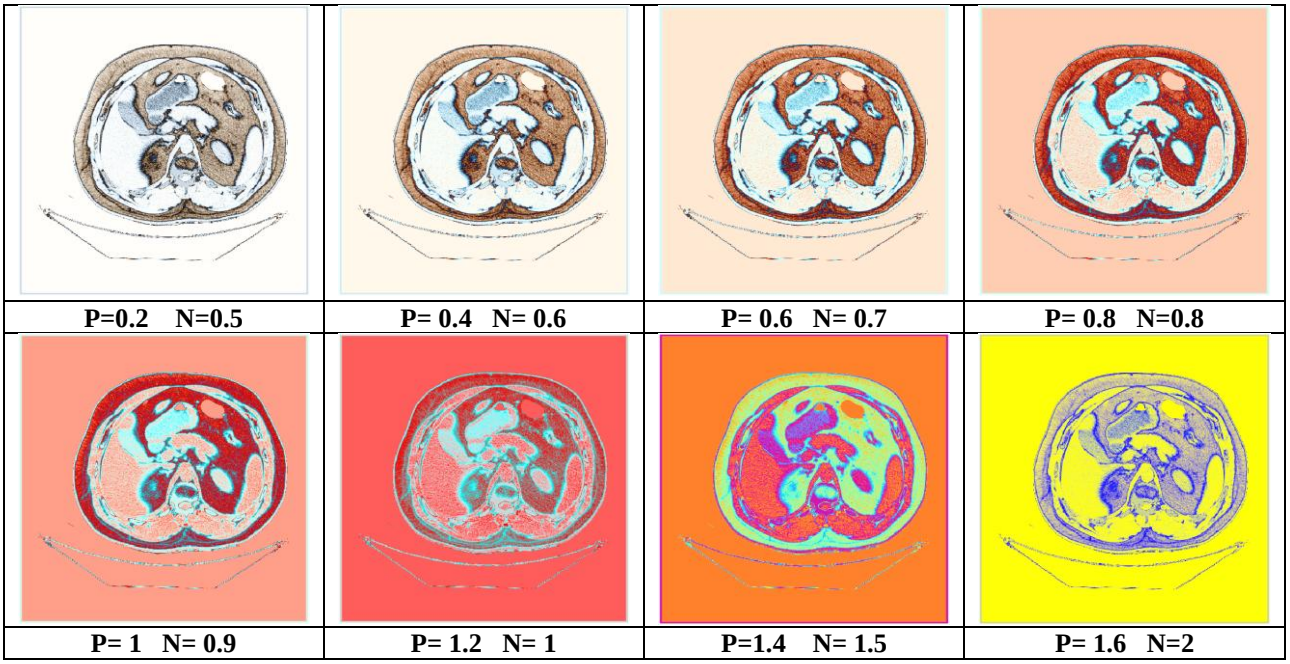

Fig.14 The color output CT-Scan images with different P and N values

ISSN: 2312-8135 | Print ISSN: 1992-0652
info@journalofbabylon.com | jub@itnet.uobabylon.edu.iq | www.journalofbabylon.com

ISSN: 2312-8135 | Print ISSN: 1992-0652
info@journalofbabylon.com | jub@itnet.uobabylon.edu.iq | www.journalofbabylon.com

2.7. When the three coefficients (F, P, N) are altered concurrently.

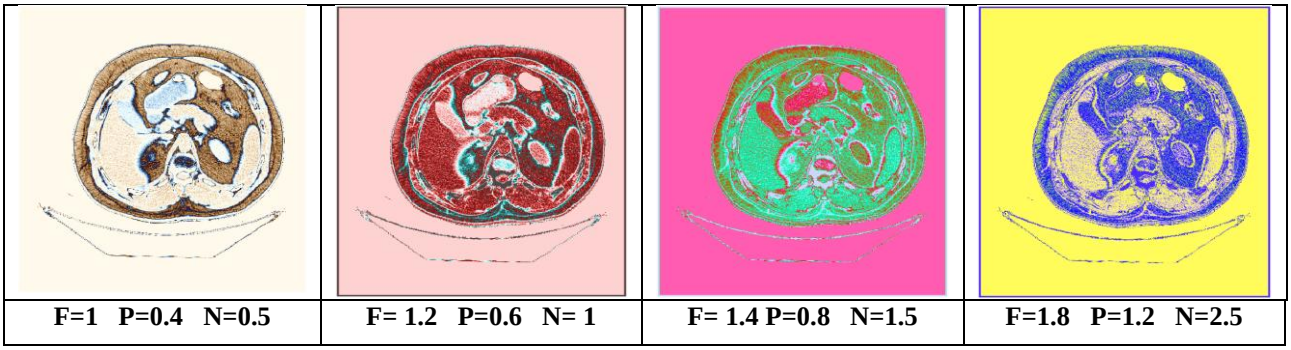

F=1 P=0.4 N=0.5	F= 1.2 P=0.6 N= 1	F= 1.4 P=0.8 N=1.5	F=1.8 P=1.2 N=2.5

Fig.15 The color output CT Scan images with different F, P, and N values

Table (8) Quality Metrics for CT-Scan when the change coefficient F

IMQ	F=0.2	F=0.3	F=0.4	F=0.5	F=0.6	F=0.7	F=0.8
PSNR	1.51327	1.707853	1.729936	1.879515	2.009266	1.885894	1.939864
ESSIM	0.98981	0.98989	0.98993	0.98984	0.98989	0.99002	0.98997
E_O	3.8463	3.84633	3.84633	3.84633	3.84633	3.84633	3.84633
E_E	3.61511	3.75262	3.75015	3.64694	3.81115	3.50263	3.60116

Table (9) Quality Metrics for CT-Scan when the change coefficient N

IMQ	N=0.1	N=0.2	N=0.3	N=0.4	N=0.6	N=0.7	N=0.8	N=0.9
PSNR	1.96448	1.96448	1.96448	1.964483	1.96448	1.96448	1.96448	1.96448
ESSIM	0.98981	0.98981	0.98981	0.98981	0.98981	0.98981	0.98981	0.98981
E_O	3.84633	3.84633	3.84633	3.84633	3.84633	3.84633	3.84633	3.84633
E_E	3.59451	3.59451	3.59451	3.59451	3.59451	3.59451	3.59451	3.59451

Table (10) Quality Metrics for CT-Scan when the change coefficient P

IMQ	P=0.3	P=0.4	P=0.5	P=0.6	P=0.7	P=0.8	P=0.9	P=1
PSNR	2.19691	2.53238	2.94756	3.48998	4.09952	4.82914	5.697754	6.72278
ESSIM	0.98976	0.98979	0.98979	0.98979	0.98978	0.98982	0.989844	0.98987
E_O	3.84633	3.84633	3.84633	3.84633	3.84633	3.84633	3.846326	3.84633
E_E	3.57414	3.59927	3.633508	3.63305	3.65885	3.67887	3.666491	3.64654

Table (11) Quality Metrics for CT-Scan when changing the coefficient F, N

IMQ	F=0.3 N= 0.1	F= 0.4 N= 0.2	F=0.5 N=0.3	F=0.6 N=0.4	F=0.7 N=0.6	F=0.8 N=0.7	F= 0.9 N=0.8	F=1 N=0.9
PSNR	1.70785	1.72994	1.87952	2.00927	1.88589	1.93986	1.96448	2.00163
ESSIM	0.98989	0.98993	0.98984	0.98989	0.99002	0.98997	0.98981	0.98973
E_O	3.84633	3.84633	3.84633	3.84633	3.84633	3.84633	3.84633	3.84633
E_E	3.75262	3.75015	3.64694	3.81115	3.50263	3.60116	3.59451	3.48103

ISSN: 2312-8135 | Print ISSN: 1992-0652
info@journalofbabylon.com | jub@itnet.uobabylon.edu.iq | www.journalofbabylon.com

Table (12) Quality Metrics for CT-Scan when change coefficient F, P

IMQ	F=1 P=0.4	F=1.2 P=0.6	F=1.4 P=0.8	F=1.6 P=1	F=1.8 P=1.2	F=2 P=1.4	F=2.2 P=1.6	F=2.4 P=1.8
PSNR	2.60091	3.41439	4.80803	5.44564	7.39318	8.17287	9.71289	8.52902
ESSIM	0.98971	0.98996	0.98978	0.98978	0.98991	0.98965	0.99009	0.98981
E_O	3.84633	3.84633	3.84633	3.84633	3.84633	3.84633	3.84633	3.84633
E_E	3.41159	3.65144	3.61515	3.54227	3.60499	3.51029	3.49146	3.58452

Table (13) Quality Metrics for CT-Scan when changing the coefficient N, P

IMQ	P=0.2 N=0.5	P= 0.4 N= 0.6	P=0.6 N=0.7	P=0.8 N=0.8	P=1 N= 0.9	P=1.2 N= 1	P=1.4 N= 1.5	P= 1.6 N=2
PSNR	1.96448	2.53238	3.48998	4.82914	6.72278	9.07959	10.8503	10.2500
ESSIM	0.98981	0.98979	0.98979	0.98982	0.98988	0.98992	0.98998	0.99001
E_O	3.84633	3.84633	3.84633	3.84633	3.84633	3.84633	3.84633	3.84633
E_E	3.59451	3.59927	3.63305	3.67887	3.64654	3.58925	3.52837	3.55834

Table (14) Quality Metrics for CT-Scan when changing the coefficient F, P, N

IMQ	F=1, P=0.4 N=0.5	F=1.2 P=0.6 N=1	F=1.4 P=0.8 N=1.5	F=1.8 P=1.2 N=2.5
PSNR	2.600908	3.414385	4.808032	7.393180
ESSIM	0.989712	0.989955	0.989777	0.989905
E_O	3.846326	3.846326	3.846326	3.846326
E_E	3.411593	3.651437	3.615148	3.604992

3. RESULTS OF COLORING CT-SCAN IMAGES FOR TANGENT FUNCTION

3.1. The parameters (N) and (P) were constant at 0.2 and 0.5, respectively, the value of the coefficient F was varied within the range of (0.2–0.8)

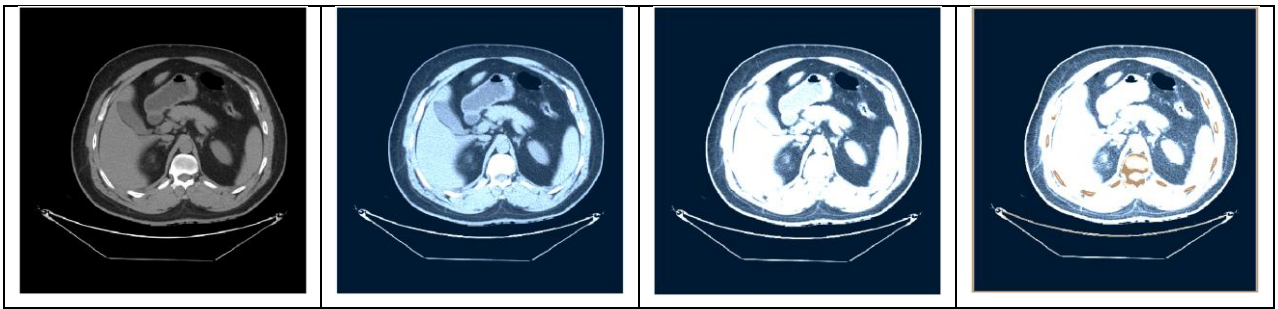

Original	F=0.2	F=0.3	F=0.4

ISSN: 2312-8135 | Print ISSN: 1992-0652
info@journalofbabylon.com | jub@itnet.uobabylon.edu.iq | www.journalofbabylon.com

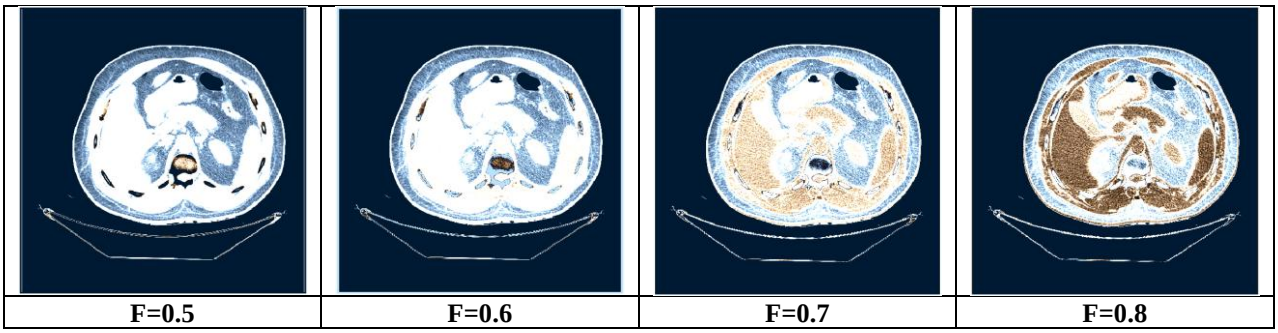

F=0.5	F=0.6	F=0.7	F=0.8

Fig.16 The color output CT-Scan images with different F values

3.2. The parameters (F), (P) were constant at 0.9 and 0.2, respectively, the value of the coefficient N was varied within the range of (0.1–0.9)

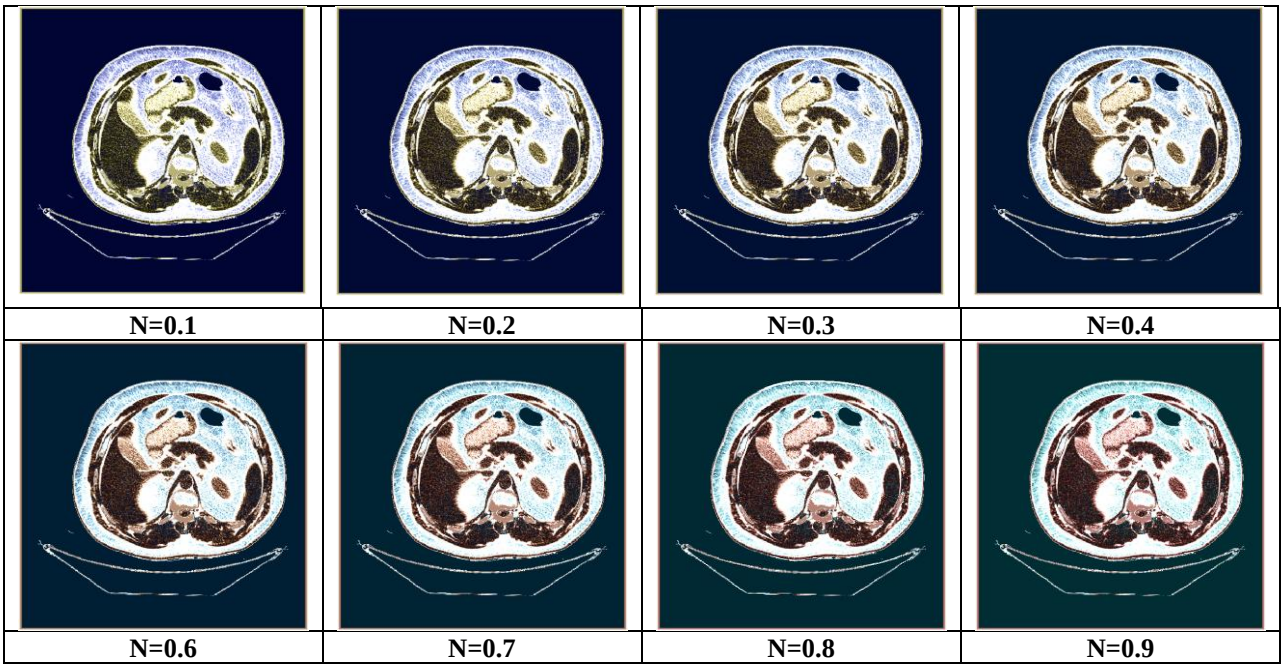

N=0.1	N=0.2	N=0.3	N=0.4
N=0.6	N=0.7	N=0.8	N=0.9

Fig.17 The color output CT-Scan images with different N values

3.3. The value of the coefficient (P) was varied within the range of (0.3–1), while coefficients F and N were kept constant at 0.9 and 0.5, respectively.

ISSN: 2312-8135 | Print ISSN: 1992-0652
info@journalofbabylon.com | jub@itnet.uobabylon.edu.iq | www.journalofbabylon.com

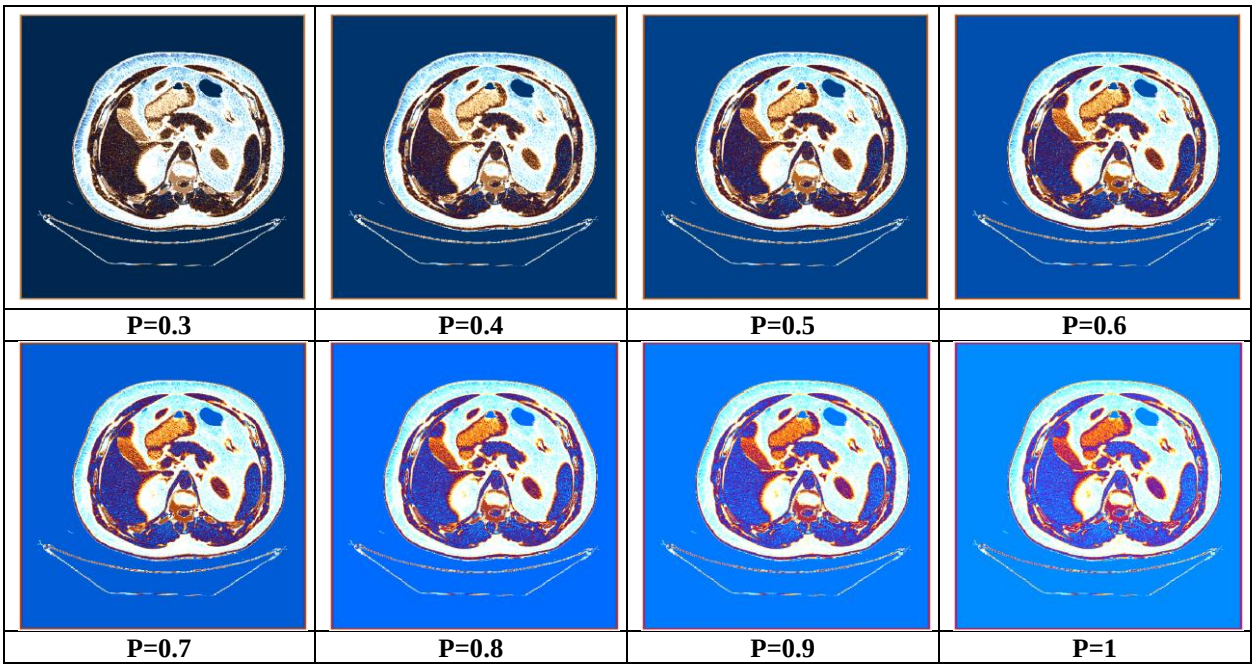

Fig.18 The color output CT- Scan images with different P value

3.4. The coefficients (F) and (N) were varied simultaneously within the ranges of (0.3–1) and (0.1–0.9), respectively, while coefficient (N) was kept constant at (0.5).

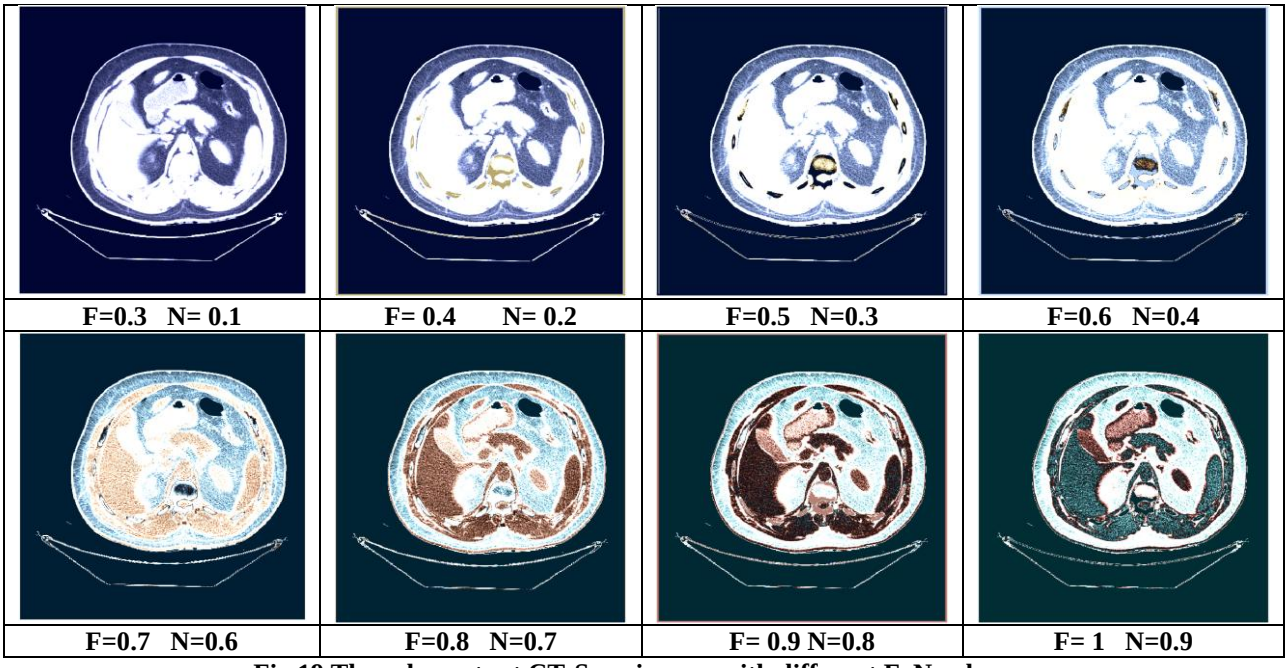

Fig.19 The color output CT-Scan images with different F, N value

3.5. When The values of coefficients F and P were adjusted across the ranges (1–2.4) and (0.4 – 1.8), while the value of coefficient (N) remained unchanged at 0.5.

ISSN: 2312-8135 | Print ISSN: 1992-0652
info@journalofbabylon.com | jub@itnet.uobabylon.edu.iq | www.journalofbabylon.com

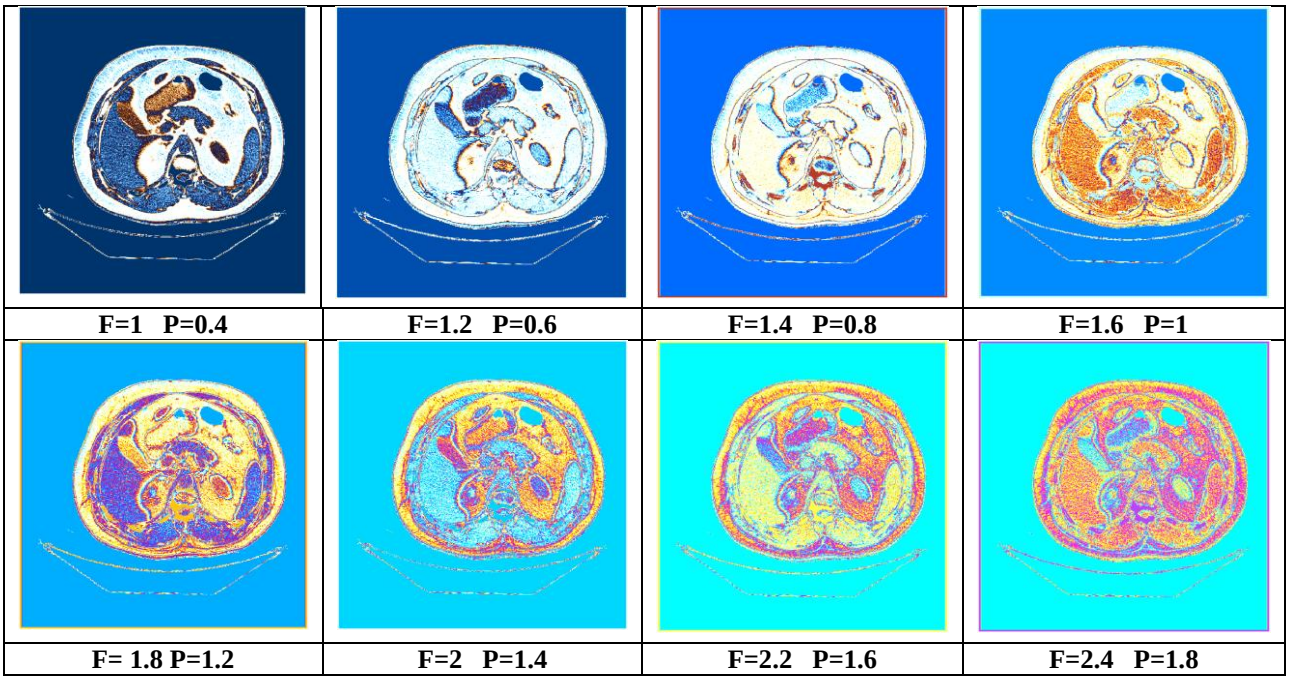

Fig.20 The color output CT-Scan images with different F, P values

3.6. Changing the values of both coefficients (N) and (P) to take a different set of values and at the same time leave the coefficient value (F) without changing, where takes the value (0.9).

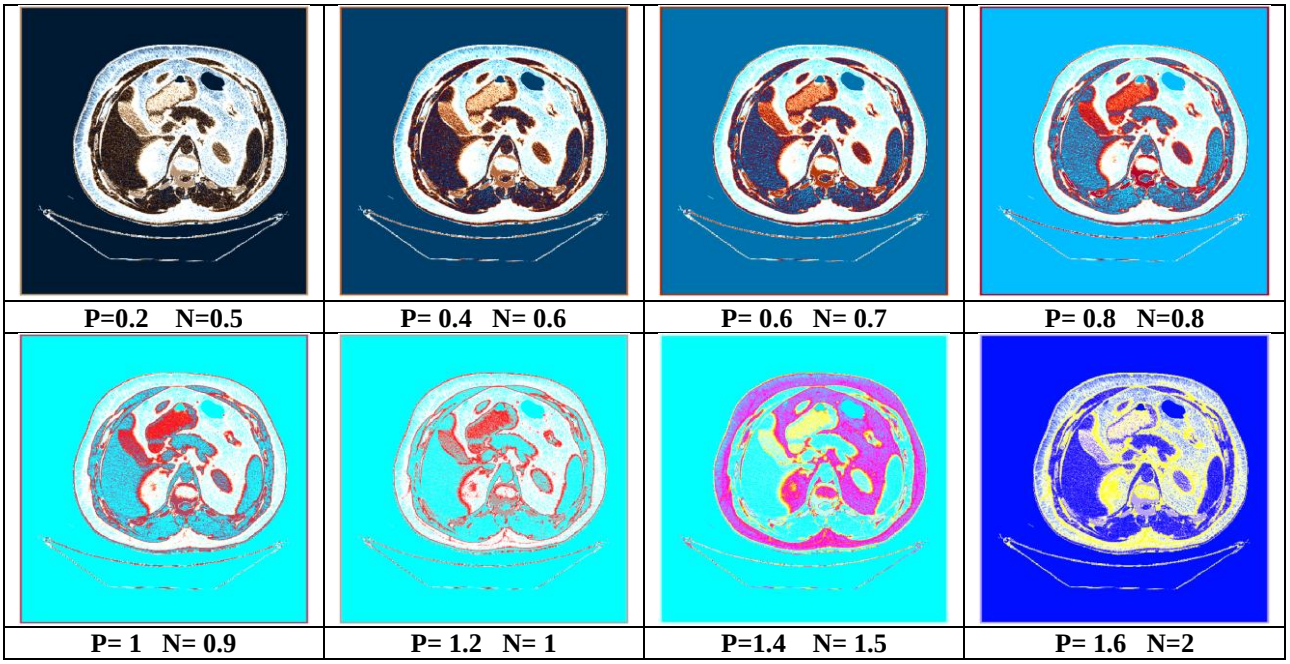

Fig.21 The color output CT-Scan images with different P and N values

مجلة جامعة بابل للعلوم الصرفة والتطبيقية مجلة جامعة بابل للعلوم الصرفة والتطبيقية

3.7. When the three coefficients (F, P, N) are altered concurrently.

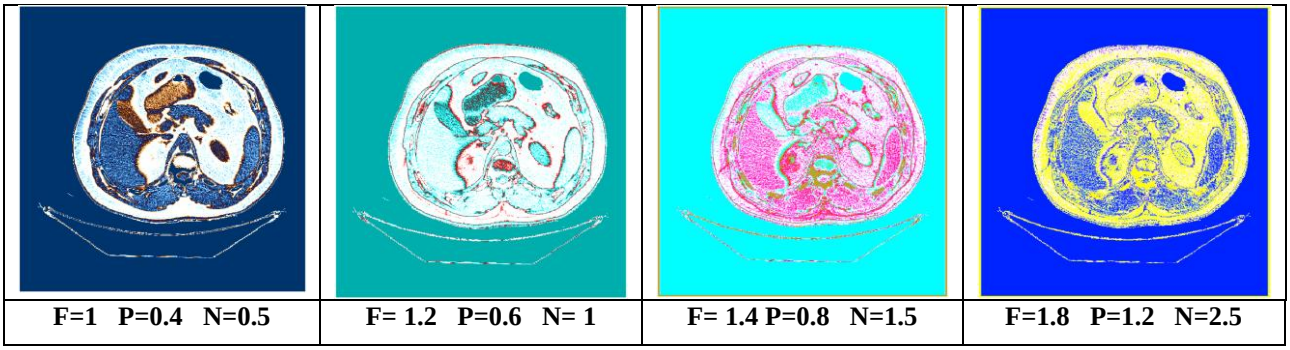

Fig.22 The color output CT-Scan images with different F, P, N values

Table (15) Quality Metrics for CT-Scan when the change coefficient F

IMQ	F=0.2	F=0.3	F=0.4	F=0.5	F=0.6	F=0.7	F=0.8
PSNR	10.88979	9.673791	8.600264	7.668417	7.713670	7.764808	7.820571
ESSIM	0.991476	0.991338	0.989636	0.992169	0.991969	0.992772	0.992000
E_O	3.846326	3.846326	3.846326	3.846326	3.846326	3.846326	3.846326
E_E	2.975385	2.423100	2.366474	2.108928	2.014905	2.285482	2.513766

Table (16) Quality Metrics for CT-Scan when the change coefficient N

IMQ	N=0.1	N=0.2	N=0.3	N=0.4	N=0.6	N=0.7	N=0.8	N=0.9
PSNR	7.37591	7.37591	7.37591	7.37591	7.37591	7.37591	7.37591	7.37591
ESSIM	0.99145	0.99145	0.99145	0.99145	0.99145	0.99145	0.99145	0.99145
E_O	3.84633	3.84633	3.84633	3.84633	3.84633	3.84633	3.84633	3.84633
E_E	2.77486	2.77486	2.77486	2.77486	2.77486	2.77486	2.77486	2.77486

Table (17) Quality Metrics for CT-Scan when the change coefficient P

IMQ	P=0.3	P=0.4	P=0.5	P=0.6	P=0.7	P=0.8	P=0.9	P=1
PSNR	6.53621	5.63559	4.65233	3.53976	2.35785	1.28108	1.29786	1.30527
ESSIM	0.99139	0.99161	0.99163	0.99172	0.99171	0.99169	0.99161	0.99156
E_O	3.84633	3.84633	3.84633	3.84633	3.84633	3.84633	3.84633	3.84633
E_E	2.68357	2.67548	2.64873	2.68256	2.68276	2.00719	1.92856	1.75434

Table (18) Quality Metrics for CT-Scan when changing the coefficient F, N

IMQ	F=0.3 N= 0.1	F=0.4 N=0.2	F=0.5 N=0.3	F=0.6 N=0.4	F=0.7 N=0.6	F=0.8 N=0.7	F=0.9 N=0.8	F= 1 N=0.9
PSNR	9.67379	8.60026	7.66842	7.71367	7.76481	7.82057	7.37591	7.32935
ESSIM	0.99134	0.98964	0.99217	0.99197	0.99277	0.99200	0.99145	0.99128
E_O	3.84633	3.84633	3.84633	3.84633	3.84633	3.84633	3.84633	3.84633
E_E	2.42310	2.36647	2.10893	2.01491	2.28548	2.51377	2.77486	2.62287

ISSN: 2312-8135 | Print ISSN: 1992-0652
info@journalofbabylon.com | jub@itnet.uobabylon.edu.iq | www.journalofbabylon.com

ISSN: 2312-8135 | Print ISSN: 1992-0652

info@journalofbabylon.com | jub@itnet.uobabylon.edu.iq | www.journalofbabylon.com

Table (19) Quality Metrics for CT-Scan when changing the coefficient F, P

IMQ	F=1 P=0.4	F=1.2 P=0.6	F=1.4 P=0.8	F=1.6 P=1	F=1.8 P=1.2	F=2 P=1.4	F=2.2 P=1.6	F=2.4 P=1.8
PSNR	5.90003	3.65214	1.21007	1.52608	1.55019	1.74463	1.63442	1.65204
ESSIM	0.99123	0.99211	0.99188	0.99303	0.99144	0.99128	0.99471	0.99202
E_O	3.84633	3.84633	3.84633	3.84633	3.84633	3.84633	3.84633	3.84633
E_E	2.45335	1.76909	1.29626	2.14931	2.49693	1.91538	2.30614	2.23945

Table (20) Quality Metrics for CT-Scan when changing the coefficient N, P

IMQ	P=0.2 N=0.5	P=0.4 N=0.6	P= 0.6 N=0.7	P=0.8 N=0.8	P=1 N=0.9	P=1.2 N=1	P=1.4 N=1.5	P=1.6 N=2
PSNR	7.37591	5.63559	3.53976	1.28108	1.30527	1.32850	1.37439	1.45428
ESSIM	0.99145	0.99161	0.99172	0.99169	0.99156	0.99152	0.99213	0.99467
E_O	3.84633	3.84633	3.84633	3.84633	3.84633	3.84633	3.84633	3.84633
E_E	2.77486	2.67548	2.68256	2.00719	1.75434	1.48727	1.44464	1.39436

Table (21) Quality Metrics for CT-Scan when changing the coefficient F, P, N

IMQ	F=1, P=0.4, N=0.5	F=1.2, P=0.6, N= 1	F= 1.4 P=0.8 N=1.5	F=1.8, P=1.2, N=2.5
PSNR	5.900032	3.652143	1.210074	1.550188
ESSIM	0.991229	0.992113	0.991877	0.991442
E_O	3.846326	3.846326	3.846326	3.846326
E_E	2.453349	1.769090	1.296258	2.496928

8. DISCUSSION

Experimental findings demonstrate that the application of three distinct mathematical functions, combined with parameters F, P, and N, to computed tomography (CT) images markedly affects image quality, as elaborated in the section following:

A. Sine function

1. When parameters N and P are held constant while parameter F is modulated in abdominal CT scans, the anatomical authentic structure remains preserved, with changes occurring strictly in color representation and gradients. Originally, a conventional grayscale display with white osseous structures and gray tissues soft, low F values introduces a dark blue background with white bones and light gray organs. As F increases, soft tissues transition from bluish – gray to a lighter gray while bone structures evolve through white and beige, finally black tones. thereby improving visual separation and delineating organ boundaries more distinctly.
2. When the coefficient N is varied while holding the other parameters fixed leads to a gradual chromatic evolution in CT images. Where the magnitude is low, the internal organs are of contrasting colours from dark green and burnt brown for the liver and spleen to light beige tones for the gallbladder, stomach, and kidneys, with well-defined white vertebrae and ribs, thus allowing strong contrast without distortion. With increasing N, the background becomes deeper green and saturation increases such that liver and spleen appear as a darker, more uniform brown with a concurrent visual enhanced distinction between kidneys and stomach while maintaining vertebral visibility.

ISSN: 2312-8135 | Print ISSN: 1992-0652 | www.journalofbabylon.com | jub@itnet.uobabylon.edu.iq | info@journalofbabylon.com

مجلة جامعة بابل للعلوم الصرفة والتطبيقية | مجلة جامعة بابل للعلوم الصرفة والتطبيقية

3. By changing the value of P with fixed F and N, chromatic systematic variations in CT images can be generated. For a low P value (0.3–0.6), the images have a dark blue background with clear organ contrast, and it can be seen that the liver and spleen are dark brown, gall bladder and stomach are beige, kidney shows well-defined light-beige tone, vertebrae are bright white with transparent colorization, preserving the anatomical structure of organs adequately. When P raises to intermediate values (0.7–1), the background gets brighter, and organ saturation intensifies, rendering the liver and spleen a denser dark brown and highlighting the kidneys and vertebrae effectively; however, although this stage makes it easier to see solid organs, the ribs' clarity starts to deteriorate as they turn brown.

4. A progressive chromatic evolution is produced in CT images by varying parameters F and N while keeping coefficient P constant. Low values display a black background with vertebrae and ribs changing from white to a range of beige, black, and gray, as well as soft tissues that are light white or pale gray in color. Darker tones seep into the soft tissues as F and N reach intermediate values, causing the stomach and gallbladder to change into beige to brown gradients, while the vertebra shifts from black to white, and the ribs transition into mixed.

5. In keeping a constant value of coefficient N, and modulating parameters F and P, a large chromatic and structural degradation is observed within experimental rows. In the first row, where the F and P values are low, the organs start out looking dark blue and brown, but then change to orange. At the beginning, the anatomical boundaries are clear and distinct, but they start to blend together as the granularity becomes more visible. The chromatic intensity rises in the second row, becoming a combination of yellow, purple, blue, and orange. At this stage, the colorization becomes excessively saturated, leading to the appearance of chromatic noise and unintended alterations in the structural representation of the organs.

6. When you change the values of parameters P and N for a given value of F, the chromatic landscape changes in a specific way. In the first stage, the drawings of anatomical forms are delineated in deep brown, turquoise, and dusky red against a progressively changing background from black to turquoise that is guaranteed not to blur out organ boundaries or lose effective contrast. As coefficients get to the mid-range levels, the background becomes filled with bright sky-blue and azure colours, while organs exhibit a variety of colours, like pale cyan for the left kidney. But then the erotic idyll becomes less clear-cut as it becomes more chromatically saturated.

7. Cofactors F, P, and N are simultaneously modulated to produce rapid changes in chromatic appearance within the visual scene from deep blue, cyan, light green, and dark blue. The anatomic margins of the liver and spleen are initially well-preserved; however, as oversaturation increases, their visual definition and visibility become diminished. The level of resolution drop is even more profound in the gastric region with increasing visual noise and saturation, which overwhelm fine anatomical features, leading to severe morphological deformation.

B. Cosine function

1. If you change the F coefficients while keeping N and P fixed/constant, you will see a slow transformation of the shape of the abdominal cross-section. In the top row, from F=0.2 to F=0.4, we observe a white image with a faint brown or beige cast. At first, the contrast between colors is not great enough to see subcutaneous layers of fat. When it changes to beiges and dark browns, it is an even more noticeable difference. Then, in the second row (0.5 −0.8) a blue-grey cast is also emerging, and on the following rows, no brown tint can be observed anymore. This reorientation turns the liver, spleen, and aorta deep blue to shades of gray. The gallbladder, as

ISSN: 2312-8135 | Print ISSN: 1992-0652 | www.journalofbabylon.com | jub@itnet.uobabylon.edu.iq | info@journalofbabylon.com

well as the stomach, turns from brown to blue. The darker colors of the organs make them more easily distinguishable from the lighter fat tissue surrounding them. Meanwhile, the ribs remain clearly visible, and the central vertebra stands out with strong contrast.

2. When you vary the value of the coefficient N while maintaining the same values for the coefficients F and P, the first row, which represents values N=0.1 to N=0.4, displays very light colors tending towards gray. The adipose tissue appears beige, the bony vertebra appears beige-brown, and the stomach and gallbladder appear as lighter regions with distinct boundaries. The left kidney, liver, and spleen remain white, and the ribs appear as if they are slightly merged. In the second row, which represents a phase of biological contrast for values N=0.6 to N=0.9, the soft tissues such as the liver and spleen remain white against a white background. However, the fat and muscle tissues appear reddish-brown. This causes the gallbladder and stomach to appear more prominent as they are gray. The vertebra appears mostly brown, making it more prominent than the ribs, which fade away compared to the previous phase.
3. When you change the value of coefficient P while keeping coefficients F and N the same, the first row, where P ranges from 0.3 to 0.6, displays a very light-yellow background color. The liver, spleen, left kidney, gallbladder, and stomach appear in white with distinct boundaries, making it possible to clearly distinguish these organs from the dark brown area surrounding them. In the second row, where P ranges from 0.7 to 1.0, the color of the background changes to gold. The kidneys and spleen seem in color pale yellow, and the stomach and gallbladder are clearly visible in sky blue color.
4. Modulating parameters F and N while keeping P the same, you get faint images with poor contrast at first, where black vertebrae and ribs stand out. Then, soft tissues shift to dark colors that make organs stand out, but some values make the image too dark and lose detail. In the higher range (F=0.7–1, N=0.6–0.9), a good white background makes organs stand out in vivid sky-blue or turquoise, with strong clarity for the stomach and kidney. Brown adipose tissue adds contrast, while the ribs fade and blend in with nearby tissues.
5. Figure (13) includes successive coloured CT-scan images that illustrate the influence of changing the F and P-coefficients (and keeping N constant). Low values are an orange colour gradient background, brown adipose tissue, sky blue organs, and black bone. But the following photos are shaded with dark browns, which creates less contrast and eventually blurs when darker colours overshadow fine details. The second row displays backgrounds from dark, golden-yellow, and more orange. The organs transform into a palette of mixed tones, with chromatic stains and fillings that do not allow the colors to be uniform. This is not due to the tissue properties, but rather the fact that the colors are overly saturated.
6. The first row represents a satisfactory stage of tissue differentiation when the parameter F remains fixed while N and P are varied. The background gradually shifts from white to a light orange tone, and the skeletal outlines remain well defined, although the edges of the ribs become less distinct. The adipose tissue and vertebrae transition from beige to red hues, clearly contrasting with the sky-blue coloration observed in the stomach and gallbladder. In contrast, the second row indicates the onset of visual distortion. The background colors shift from golden orange and bright yellow to violet and intense yellow tones. Although the skeletal structures are still discernible, the soft tissues undergo noticeable color changes, adopting violet and strong yellow shades. At this stage, small punctate artifacts and chromatic irregularities begin to appear, disrupting the uniform appearance of the tissues.
7. Figure (15) illustrates the rapid transition from clear color representation to noticeable distortion when the parameters F, P, and N are varied simultaneously. In the initial stage, corresponding

ISSN: 2312-8135 | Print ISSN: 1992-0652

info@journalofbabylon.com | jub@itnet.uobabylon.edu.iq | www.journalofbabylon.com

to lower parameter values, the image exhibits well-defined tissue differentiation without visible noise. The adipose tissue appears brown, the organs display beige tones, and the stomach and gallbladder are represented in a light blue-gray color, allowing clear visual separation. In the second stage, between intermediate values of parameters, one can see a slow chromatic shift towards red as well as the appearance of artifacts. It causes most tissue to appear to be a dark red color, which in turn impedes the visualization of boundaries and differentiation. The stomach and gallbladder are still recognizable, appearing as a pale red structure.

C. Tangent function

1. Changing the coefficient (F) while keeping (N) and (P) the same at first causes a phase of too much brightness to start at (F=0.2). This phase has a dark blue background and soft tissues that go from cyan to white and lose their boundaries, internal texture, and contrast between bone and tissue. As move to the second row, the F value goes up, giving the image a brown-gold tone. However, at F values of 0.7 and 0.8, high brightness and distortion continue, and granular noise appears, which makes it harder to see thoracic bone details and makes the image less clear overall, even though it does make the texture of the organs stand out a little more.
2. Changing the coefficient N (keeping coefficients P and F unchanged). No large difference in attenuation characteristics (0.1-0.4) background is not change much, while soft tissue appears sharply as a yellow-olive colored one by conditional factor value down to moderate hepatic texture & clear vertebral definition, but rib was less apparent. At the high end of the range (N=0.6 to N=0.9), the background transitions toward dark green, and organs take on a brown color with much greater definition around organ edges and sharper edges for the external borders of both liver and gallbladder, which results in a phase that looks visually balanced with no apparent strain or oversaturation in color while still providing differentiation between structures.
3. Varying coefficient P while keeping F and N constant produces noticeable visual changes across two distinct phases. In the first range (0.3–0.6), the background shifts from dark indigo to a lighter tone, enhancing contrast. The liver and spleen appear brown, the gallbladder is clearly visible in orange without losing its boundaries, and the vertebra remains well defined in white with a light brown thoracic point. Once we start to get levels that are increasing between 0.7 and one, the background goes into a stronger blue color, and the tissue color becomes affected as well." The gallbladder and stomach change from brown to red-orange, the liver and spleen from brown to greenish-blue. The bones of the vertebral column and thoracic cage remain white and brown, respectively.
4. The first row of Figure (19) in which P is constant and F and N are played with, becomes darker (blue), going from (F=0.3, N=0.1) to (F=0.6, N=0.4), and shows white/gray gradients in tissue regions. It transforms the shape of the liver, spleen, stomach, and gallbladder into bright white masses that conceal their texture within. In the second row from (F = 0.7, N = 0.6) to (F = 1, N = 0.9), the background becomes green, and organs become granular with mixed colours such as beige or brown. The aorta is kept clear, and the liver and gall bladder can be discerned. The vertebral limits are initially difficult to trace, and become white, whereas the points of the thoracic cage remain untraceable due to polychromatic variability.
5. The figure (20) illustrates the simultaneous adjustment of the coefficients (F and P) while N remains constant. As seen in the first row of the figure, where F changes from 1 to 1.6, and P changes from 0.4 to 1, the initial image at F = 1 and P = 0.4 shows a markedly dark blue background, where the vertebra appears bright white, and the liver appears dark blue. The

ISSN: 2312-8135 | Print ISSN: 1992-0652

info@journalofbabylon.com | jub@itnet.uobabylon.edu.iq | www.journalofbabylon.com

details of the gallbladder are clearly superimposed in brown. The aorta is also clearly visible as a blue circle in front of the vertebra. The spleen also appears blue, and the stomach appears light brown. This initial image appears to be clearer than the subsequent images in this row, which show vivid and divergent coloration for both background and organs. This results in significant distortion and obscuration of tissue details, especially in the final images, where vivid coloration and granularity have resulted in complete distortion, making it impossible to differentiate any organ or bone.

6. The first row (P=0.2/N=0.5 to P=0.8/N=0.8) changes from a dark background with brown organs to an azure setting with brick-red tissues. The vertebra, aorta, and gallbladder are still clearly separated, but the thoracic bones change from beige to red. In the second row (P=1/N=0.9 to P=1.6/N=2), the background changes from blue to dark indigo, and the organs turn bright yellow. This results in a loss of the internal details and bone boundaries because the brightness becomes too high, even though the outer edges of the organs remain visible.

7. Sequential changes in the F, P, and N coefficients cause progressive loss of diagnostic image quality. The parameter configuration (F=1, P=0.4, N=0.5) yielded the most diagnostically favorable result, providing optimal contrast between the dark blue background, the brown gallbladder, and the white vertebral structures. in contrast the second configuration (F=1.2, P=0.6, N=1) has given a turquoise coloration. While the border between the tissue and osseous structure is well defined, internal tissue structures and osseous structures become less visible with increased brightness. The third set, F=1.4, P=0.8, and N=1.5, reveals brightening with the pink color that completely disguises liver–gallbladder interface (the interfacial boundary) and vertebral structure. In the final F=1.8, P=1.2, and N=2.5 combination, there is a full color inversion with dark-indigo in the background against bright-yellow for structures that obscure differentiation between them all together.

● Medical Image Quality

The experimental results presented in Tables (1-21) demonstrate the efficiency of the proposed coloring algorithm using the three functions. These results show that the F-factor controls the contrast, while the P-factor has the most significant impact on altering the image's color properties. The N-factor exhibits a limited effect on the algorithm. The behavior of the metrics can be discussed within the following scientific framework:

1. Signal-to-Noise Ratio (PSNR) Measurement: This measure assesses the difference between the original and colored images .The tables show variations in PSNR values, decreasing in some cases and increasing in others (especially when the P-factor is changed). This variation in the context of coloring is interpreted as a natural consequence of converting the image from grayscale to color. Since PSNR measures the numerical difference between the pixels of the grayscale image and the resulting colors, any effective coloring will inevitably result in a large numerical difference (and therefore a low PSNR). Thus, the decrease in values in the Sin tables and the increase in some Cos tables reflect how the trigonometric function shifts pixel values to achieve a color contrast easily discernible to the human eye.
2. The Structural Similarity Identification Scale (ESSIM) measures the preservation of anatomical structure and edges, its values showed high stability, approximately 0.99, across various parameter settings (F, N, P) for all three functions. This mathematically proves that the coloring process did not alter the structural or anatomical features of the image (such as tissue boundaries

ISSN: 2312-8135 | Print ISSN: 1992-0652 | jub@itnet.uobabylon.edu.iq | www.journalofbabylon.com | info@journalofbabylon.com

or tumor outlines). The value remaining close to 1 indicates that the coloring is a visual enhancement and does not affect the original data.

3. The Entropy Scale measures the information content of the image. The tables show that the entropy of the colored image (E_E) is slightly less than or equal to the entropy of the original image (3.84). This decrease or stability indicates that the coloring process successfully focused the information by reducing the visual randomness resulting from closely spaced grayscale gradations through their organization into specific color ranges. This makes it easier for the human eye to isolate tissues without loss of the image's informational core.

The enhanced images were presented to two radiology specialists, who evaluated the image quality from a visual perspective. The results were evaluated by Dr. Thamer Jassim Al-Mousawi and Dr. Inas Abdul-Hussein Mahdi, both specialists in diagnostic radiology. Although some objective metrics, such as PSNR and entropy, may not show a significant improvement in the results, the visual assessment by radiology experts indicated an improvement in the clarity of visual details and the perceptual quality of many images in the previous tables. This indicates that objective metrics alone may not fully reflect the visual enhancements in medical image colorization applications, and that visual assessment can provide a complementary perspective to quantitative evaluation.

9. CONCLUSION

The primary objective of such an algorithm is to enhance the medical image by enhancing its quality: increasing the contrast or brightness, bringing out interesting features, and removing imaging artifacts. This contributes to the precision diagnosis and therapy for different diseases. This paper presents a mathematical colorization method with three mathematical functions by using three fundamental parameters and, subsequently, applies it to CT images under different parameters. The findings demonstrate that modifications to the three mathematical parameters have different effects, resulting in numerous colorizations of organs and surrounding tissues. The contrast is thus improved, and we get better insight into the quality of the image. There was deformation due to saturation effects, but the presence of moderate coloring is needed for better performance.

Conflict of interests.

There are non-conflicts of interest.

References

[1] W. Wei, B. Zhou, D. Połap, and M. Woźniak, "*A regional adaptive variational PDE model for computed tomography image reconstruction,*" Pattern Recognit., vol. 92, pp. 64–81, 2019.

[2] M. Kaur and M. Singh, "*Contrast enhancement and pseudo coloring techniques for infrared thermal images,*" in Proc. 2018 2nd IEEE Int. Conf. Power Electron., Intell. Control Energy Syst. (ICPEICES), Delhi, India, pp. 1005–1009, 2018.

[3] S. Moradzadeh and V. Mehrdad, "*Improvement of medical images with multi-objective genetic algorithm and adaptive morphological transformations*," Sci. Rep., vol. 15, no. 1, Art. No. 24167, 2025.

[4] B. Selvapriya and B. Raghu, "*Enhancement of medical images using various pseudo coloring techniques*," Int. J. Recent Technol. Eng. (IJRTE), vol. 7, no. 6S3, p. 117, 2019.
[5] A. A. Raji, O. I. Adebisi, A. O. Akinola, and B. A. Ogundare, "*Bimodal technique for enhancement of picture quality of medical images*," ITEGAM-JETIA, vol. 11, no. 53, pp. 177–185, 2025.
[6] G. Dougherty, Ed., *Medical Image Processing: Techniques and Applications*. New York, NY, USA: Springer, 2011.
[7] B. Selvapriya and B. Raghu, "*Colorization using desired color for medical images*," Int. J. Recent Technol. Eng., vol. 7, no. 6S3, pp. 124–132, 2019.
[8] M. M. Hadhoud, "*Image coloring techniques and applications*," Ph.D. dissertation, Menoufia Univ., Menoufia, Egypt, 2011.
[9] M. U. G. Khan, Y. Gotoh, and N. Nida, "*Medical image colorization for better visualization and segmentation,*" in Proc. Annu. Conf. Med. Image Understand. Anal. (MIUA), Cham, Switzerland, pp. 571–580, 2017.
[10] S. M. S. Islam, M. A. A. Nasim, I. Hossain, D. M. A. Ullah, D. K. D. Gupta, and M. M. H. Bhuiyan, "*Introduction of medical imaging modalities*," in Data Driven Approaches on Medical Imaging. Cham, Switzerland: Springer Nature, pp. 1–25, 2023.
[11] D. Kumar, B. Pratap, N. Boora, R. Kumar, and N. K. Sah, "*A comparative study of medical imaging modalities*," Int. J. Radiol. Sci., vol. 3, no. 1, pp. 9–16, 2021.
[12] S. Hussain et al., "*Modern diagnostic imaging technique applications and risk factors in the medical field: A review*," BioMed Res. Int., vol. 2022, no. 1, Art. No. 5164970, 2022.
[13] D. J. Brenner and E. J. Hall, "*Computed tomography—An increasing source of radiation exposure*," N. Engl. J. Med., vol. 357, no. 22, pp. 2277–2284, 2007.
[14] Gonzalez, R. C., & Woods, R. E. (2018). Digital image processing 4th edition. *Pearson*.
[15] Z. Zhang, "*Review on the application of machine learning in medical image*," 2025.
[16] Memon, F., Unar, M. A., & Memon, S. (2015). Image quality assessment for performance evaluation of focus measure operators. Mehran University Research Journal of Engineer
[17] Sara, U., Akter, M., & Uddin, M. S. (2019). Image quality assessment through FSIM, SSIM, MSE and PSNR—a comparative study. *Journal of Computer and Communications*, *7*(3), 8-18.
[18] Al-Hilo, E.," Speeding-up Fractal Colored Image Compression using Moments Features, PHD Theses ,2007.
[19] Kuppusamy, P. G., Joseph, J., & Sivaraman, J., "A full reference morphological edge similarity index to account processing induced edge artefacts in magnetic resonance images". Biocybernetics and Biomedical Engineering, Vol.37, No.1,pp.159-166.,2017.
[20] Sulaiman, S., & Hanapi, Z. M.," Extensive Analysis on Images Encryption using Hybrid Elliptic Curve Cryptosystem and Hill Cipher". University of Putra Malaysia, Serdang, Selangor, Malaysia, Vol.17, No.3, pp.221.230,2021.

ISSN: 2312-8135 | Print ISSN: 1992-0652
info@journalofbabylon.com | jub@itnet.uobabylon.edu.iq | www.journalofbabylon.com
مجلة جامعة بابل للعلوم الصرفة والتطبيقية مجلة جامعة بابل للعلوم الصرفة والتطبيقية

الخلاصة

أدى التقدم السريع في التقنيات الطبية الى زيادة كبيرة في الحصول على الصور الطبية وتخزينها ,لاسيما تقنيات مثل التصوير المقطعي المحوسب (CT) يسلط هذا التطور الحاجة الى خوارزميات فعالة لمعالجة الصور يمكنها دعم الأطباء في تشخيص الحالات الطبية وتقييمها بكفاءة اكبر , من بين هذه الأساليب ,نال تلوين الصور الطبية اهتمام متزايد على مر السنين. فعلى عكس الصور الرمادية التقليدية توفر الصور الملونة المصنعة معلومات بصرية محسنة عن الاعضاء والأنسجة مما يحسن تفسير الصور .في هذه الدراسة تم اقتراح نهج رياضي جديد لتحسين جودة صور الاشعة المقطعية بأستخدام الدوال المثلثية التي تحكمها ثلاثة معايير رئيسية بأستخدام برنامج الماتلاب. تظهر النتائج التجريبية أن تحسين تباين الألوان يساهم في تمييز أكثر دقة بين الأنسجة والأعضاء المختلفة مما يوفر تمثيلا بصريا واضحا ويدعم العمليات التحليلية والتشخيصية. وأشار تقييم خبراء الأشعة إلى تحسن ملحوظ في جودة الصور المحسّنة، مما يدعم نتائج التقييم الكمي ويؤكد فعالية الطريقة المقترحة.

ISSN: 2312-8135 | Print ISSN: 1992-0652
info@journalofbabylon.com | jub@itnet.uobabylon.edu.iq | www.journalofbabylon.com